The Plant Cell, Vol. 11, 2167–2185, November 1999, www.plantcell.org © 1999 American Society of Plant Physiologists

Peroxisomal Membrane Ascorbate Peroxidase Is Sorted to a Membranous Network That Resembles a Subdomain of the Endoplasmic Reticulum

Robert T. Mullen,[a,1] Cayle S. Lisenbee,[a] Jan A. Miernyk,[b,2] and Richard N. Trelease[a,3]

[a] Department of Plant Biology and Graduate Program in Molecular and Cellular Biology, Arizona State University, Tempe, Arizona 85287-1601

[b] U.S. Department of Agriculture, Agricultural Research Service, National Center for Agricultural Utilization Research, Peoria, Illinois 61604-3902

The peroxisomal isoform of ascorbate peroxidase (APX) is a novel membrane isoform that functions in the regeneration of NAD^+ and protection against toxic reactive oxygen species. The intracellular localization and sorting of peroxisomal APX were examined both in vivo and in vitro. Epitope-tagged peroxisomal APX, which was expressed transiently in tobacco BY-2 cells, localized to a reticular/circular network that resembled endoplasmic reticulum (ER; 3,3′-dihexyloxacarbocyanine iodide–stained membranes) and to peroxisomes. The reticular network did not colocalize with other organelle marker proteins, including three ER reticuloplasmins. However, in vitro, peroxisomal APX inserted posttranslationally into the ER but not into other purified organelle membranes (including peroxisomal membranes). Insertion into the ER depended on the presence of molecular chaperones and ATP. These results suggest that regions of the ER serve as a possible intermediate in the sorting pathway of peroxisomal APX. Insight into this hypothesis was obtained from in vivo experiments with brefeldin A (BFA), a toxin that blocks vesicle-mediated protein export from ER. A transiently expressed chloramphenicol acetyltransferase–peroxisomal APX (CAT-pAPX) fusion protein accumulated only in the reticular/circular network in BFA-treated cells; after subsequent removal of BFA from these cells, the CAT-pAPX was distributed to preexisting peroxisomes. Thus, plant peroxisomal APX, a representative enzymatic peroxisomal membrane protein, is sorted to peroxisomes through an indirect pathway involving a preperoxisomal compartment with characteristics of a distinct subdomain of the ER, possibly a peroxisomal ER subdomain.

INTRODUCTION

Peroxisomes are found in virtually all eukaryotic cells and are delineated by a single boundary membrane. These organelles typically are involved in the generation and degradation of toxic hydrogen peroxide and the β oxidation of fatty acids; they also house a diversity of enzymes that participate in various other metabolic processes specific to the organism, cell/tissue type, or environmental conditions (Huang et al., 1983; Baker, 1996; Gietl, 1996).

Nuclear genes encode all of the protein and enzyme constituents of the peroxisomal matrix. After synthesis on polysomes in the cytosol, these proteins are targeted posttranslationally to the organelle in a regulated manner. At least two types of evolutionarily conserved peroxisomal targeting signals (PTSs) are capable of directing proteins to the peroxisomal matrix (Olsen, 1998; Subramani, 1998). The type 1 PTS (PTS1) is an uncleaved C-terminal tripeptide motif—that is, small basic hydrophobic residues—or variants thereof (Mullen et al., 1997a, 1997b), that is found in the many peroxisomal matrix–destined proteins. The type 2 PTS (PTS2) is a nonapeptide motif (R/K-X_6-H/Q-A/L/F [where X indicates any amino acid]) (Flynn et al., 1998) located in the N terminus of another set of matrix proteins that are proteolytically processed after import into peroxisomes. Proteinaceous receptors (those recognizing PTS1- and PTS2-containing proteins) and several components of the peroxisome translocation machinery have been identified in various organisms. These proteins are termed peroxins, given as Pex to describe the protein and *PEX* to describe the gene (Distel et al., 1996), and have been identified in a number of species. For instance, PTS1 receptors encoded by *PEX5* genes have been isolated from watermelon (Wimmer et al., 1998), Arabidopsis (Brickner et al., 1998), and tobacco

[1] Current address: Department of Biology, York University, Toronto, Ontario M3J 1P3, Canada.

[2] Current address: Plant Genetics Research Unit, U.S. Department of Agriculture, Agricultural Research Service, Curtis Hall, University of Missouri, Columbia, MO 65211.

[3] To whom correspondence should be addressed. E-mail trelease.dick@asu.edu; fax 480-965-6899.

(Kragler et al., 1998), and *PEX10* and *PEX16* genes have been isolated more recently from Arabidopsis (Lin et al., 1999; Schumann et al., 1999).

Details related to targeting signals and trafficking pathways for peroxisomal membrane proteins (PMPs) are beginning to emerge. PMPs are synthesized in the cytosol (with one exception, reported by Bodnar and Rachubinski, 1991) and are post-translationally targeted to peroxisomes directly or indirectly. Support for the direct insertion of PMPs comes mainly from in vitro import studies with mammalian and plant peroxisomes (Imanaka et al., 1996; Just and Diestelkötter, 1996; Tugal et al., 1999) and from in vivo targeting studies in which a deletion of the membrane peroxisomal targeting signal in *Candida boidinii* PMP47 resulted in the protein being localized exclusively in the cytosol (Dyer et al., 1996).

Other PMPs appear to be targeted to peroxisomes indirectly, that is, by way of the endoplasmic reticulum (ER), a formerly discredited pathway for peroxisome biogenesis that has now been resurrected (albeit significantly modified) by some investigators (Erdmann et al., 1997; Kunau and Erdmann, 1998; Subramani, 1998; Titorenko and Rachubinski, 1998a). Evidence for this pathway includes the pulse–chase analyses of radiolabeled rat PMP50, which revealed that this membrane protein was synthesized on membrane-bound polysomes and localized in the ER before insertion into peroxisomes (Bodnar and Rachubinski, 1991). Moreover, human PMP Pex3p and a chimeric protein composed of the N terminus of Pex3p from *Hansenula polymorpha* fused to a reporter protein both caused a profound proliferation of ER membranes when overexpressed in vivo (Baerends et al., 1996; Kammerer et al., 1998). Proliferation of ER membranes also was observed when the *Saccharomyces cerevisiae* PMP Pex15p was overexpressed. In addition, the C-terminal domain of Pex15p was O-glycosylated, indicating that this portion of the protein protruded, at least transiently, into the lumen of the ER (Elgersma et al., 1997). The indirect trafficking pathway for PMPs seems to involve participation of distinct ER-derived vesicles that contain components of coat protein II (COP II) (Titorenko and Rachubinski, 1997) and at least two Pexs (Pex1p and Pex6p) that show sequence similarity to *N*-ethylmaleimide-sensitive factor-like ATPases. All of these proteins may function during vesicle fusion with the peroxisome boundary membrane (Titorenko and Rachubinski, 1997, 1998b; Faber et al., 1998).

Our knowledge of the sorting of PMPs to the peroxisomal boundary membrane in plant cells is rudimentary. Only three authentic plant PMPs have been identified, none of which has been demonstrated to function as a Pex, that is, as a protein involved in peroxisome biogenesis. Authentic plant PMPs include a 28-kD polypeptide of unknown function (Yamaguchi et al., 1995), a putative 73-kD molecular chaperone (Corpas and Trelease, 1997), and a 30- to 31-kD isoform of ascorbate peroxidase (APX; Yamaguchi et al., 1995; Bunkelmann and Trelease, 1996). Peroxisomal APX, a constitutive component of the boundary membrane in oilseed seedling glyoxysomes and leaf (and leaf-type) peroxisomes, functions to protect the cell from toxic reactive oxygen species generated through the β oxidation of fatty acids within the organelle (Mullen and Trelease, 1996; Corpas and Trelease, 1998). cDNAs encoding peroxisomal APX have been isolated from cotton (Bunkelmann and Trelease, 1996), Arabidopsis (Zhang et al., 1997), and spinach (Ishikawa et al., 1998). The deduced amino acid sequence of peroxisomal APX reveals a high degree of identity with cytosolic APX but it has, in addition, a C-terminal 41–amino acid extension that contains a single, putative membrane-spanning region.

In this study, we describe the intracellular trafficking pathway of cottonseed peroxisomal APX in suspension-cultured tobacco BY-2 cells, a well-characterized in vivo peroxisomal import system (Banjoko and Trelease, 1995; Trelease et al., 1996a; Lee et al., 1997; Mullen et al., 1997a, 1997b; Flynn et al., 1998). Immunofluorescence microscopic analyses revealed that epitope-tagged cottonseed peroxisomal APX is sorted both to peroxisomes (glyoxysomes) and to a distinct membrane compartment with characteristics of a subdomain of the ER. Direct in vitro evidence showed that peroxisomal APX is inserted post-translationally into highly purified ER membranes but not into peroxisome membranes. Collectively, the results suggest that peroxisomal APX is sorted indirectly to peroxisomes by way of the ER, implicating this endomembrane compartment in the biogenesis of peroxisomes in plant cells.

RESULTS

Transiently Expressed, Epitope-Tagged Peroxisomal APX Is Localized to BY-2 Peroxisomes and to a Reticular/Circular 3,3′-Dihexyloxacarbocyanine-Stained Subcompartment

As with peroxisomes (glyoxysomes) in oilseed cotyledons and endosperm, peroxisomes in suspension-cultured tobacco BY-2 cells possess an endogenous membrane-bound peroxisomal APX (see below). Because immunodetection of endogenous peroxisomal APX would complicate experiments designed to elucidate the subcellular location of introduced wild-type or mutated cottonseed peroxisomal APX, a hemagglutinin (HA) epitope-tagged version of this peroxisomal APX (HA-pAPX; Figure 1) was constructed with a single copy of the HA epitope tag at the N-terminal end of the peroxisomal APX . The N terminus of peroxisomal APX was deemed a suitable location for the HA tag for several reasons: (1) preliminary data indicated that the targeting information, along with the transmembrane spanning domain, were located at the C terminus of the protein; (2) HA-tagged peroxisomal APX was inserted into membranes in vivo and in vitro (J.A. Miernyk and R.T. Mullen, unpublished data); and (3) as shown in the crystalline structure of recombinant

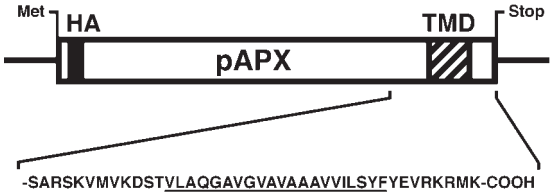

Figure 1. Schematic Representation of Cottonseed HA-pAPX.

A sequence encoding a single HA epitope tag (MGYPYDVPDYAG-underlined; depicted by solid box) was appended to the 5′ end of the cottonseed peroxisomal APX open reading frame by using the polymerase chain reaction (see Methods). The polypeptide sequence shown is for a unique C-terminal 41–amino acid extension that is not found in cytosolic APXs. This extension contains a single, putative transmembrane domain (TMD, underlined and depicted by the hatched box).

cytosolic pea APX, the N terminus protruded from the tertiary core of the polypeptide (Patterson and Poulos, 1995).

Figure 2A illustrates a representative punctate immunofluorescence pattern observed within nontransformed BY-2 cells incubated with anti-cucumber peroxisomal APX IgGs. This pattern is characteristic of antigenic proteins localized to peroxisomes (Lee et al., 1997; Mullen et al., 1997a, 1997b; Flynn et al., 1998). The subcellular location of HA-pAPX expressed transiently (its expression driven by the cauliflower mosaic virus 35S promoter) for 20 hr in a BY-2 cell is shown in Figure 2B. Immunodetection of the HA epitope on peroxisomal APX overexpressed within transformed cells revealed a substantially different immunofluorescence pattern, that is, both punctate and reticular/circular patterns. The circular structures commonly observed within this reticular pattern also are observed in nontransformed living cells (see Figure 3) and thus are not formed solely as a consequence of transient overexpression of HA-pAPX. Figure 2C illustrates in the same transformed cell the punctate immunofluorescence pattern attributable to endogenous peroxisomal catalase. In Figure 2D, the yellow/orange color of the merged images (Figures 2B and 2C) reveals that only the punctate portion of HA-pAPX fluorescence colocalizes entirely with the punctate catalase fluorescence pattern. This obvious colocalization indicates that at least some of the introduced HA-pAPX is sorted to endogenous peroxisomes. However, Figure 2D also shows that a significant portion of the introduced HA-pAPX—that in the reticular/circular structures (Figures 2B and 2D)—does not colocalize with catalase in peroxisomes. Thus, after expression for ~20 hr, introduced HA-pAPX becomes localized to at least two distinguishable subcellular compartments in BY-2 cells, namely, peroxisomes and a reticular/circular network.

Control experiments included bombardment of cells with different gene constructs. In one experiment, peroxisomal APX (lacking an N-appended HA epitope tag) was introduced biolistically; the transformed cells that were labeled with anti-peroxisomal APX IgGs and conjugated secondary antibodies exhibited both a punctate and a reticular/circular fluorescence pattern similar to that illustrated in Figure 2B (results not shown), indicating that the observed sorting of HA-pAPX was not due to the appended HA tag. In a mock transformation control, application of anti-HA IgGs and conjugated secondary antibodies yielded no immunofluorescence image (e.g., Figure 4F in Lee et al., 1997).

Elucidation of the HA-pAPX immunofluorescence pattern led to follow-up in vivo experiments aimed at determining the identity of the reticular/circular network. Specifically, HA-pAPX–transformed cells were double labeled with fluor-conjugated secondary antibodies bound to anti-HA IgGs and to IgGs raised against resident enzymes/proteins that specifically mark various plant cell organelles. Figures 2E through 2G illustrate merged confocal images of these results. In Figure 2E, reversibly glycosylated polypeptide (Dhugga et al., 1997) obviously is not colocalized with HA-pAPX, indicating that Golgi bodies are not part of the reticular/circular network to which HA-pAPX is localized. Figure 2F reveals that mitochondrial β-ATPase (Luethy et al., 1993) is distinct from the HA-pAPX reticular/circular network, as is the δ isoform of tonoplast intrinsic protein (Figure 2G) that marks one of several types of vacuoles in plant cells (Neuhaus and Rogers, 1998). Plastids detected with anti-stearoyl–acyl carrier protein Δ-9 desaturase antibody applied to BY-2 cells also did not resemble the HA-pAPX–stained network (Trelease et al., 1996a). Although the results from this series of studies provide negative evidence, the data are quite compelling that Golgi bodies, mitochondria, a vacuolar compartment, and plastids are not part of the reticular/circular network to which HA-pAPX becomes localized.

3,3′-Dihexyloxacarbocyanine iodide ($DiOC_6$) is commonly used to visualize ER, even though it often stains other membranes as well (see Discussion). Figure 3A illustrates a HA-pAPX immunofluorescence pattern, including punctate (peroxisomes) and reticular/circular structures (similar to Figure 2B), but imaged with cyanine 5 (Cy5). Figure 3B shows the results of $DiOC_6$ staining of the same cell. A reticular/circular fluorescence pattern, but not a punctate peroxisomal pattern, is observed in the transformed (and surrounding nontransformed; Figure 3D) cell. The yellow/orange color in the merged image (Figure 3C) shows substantial, but not complete, colocalization of the HA-pAPX and $DiOC_6$ patterns. This and previous results suggest that in addition to being localized to peroxisomes, HA-pAPX is localized to some part of the ER that constitutes virtually all of the reticular/circular network.

One of our concerns was that the reticular/circular network constituted an anomalous membrane compartment within biolistically transformed cells. Several observations, however, indicated that this was not the case. In Figure 3D, a representative image of two $DiOC_6$-stained, nontransformed cells in a population of bombarded cells, the reticular/circular pattern is clearly evident. As a control for the

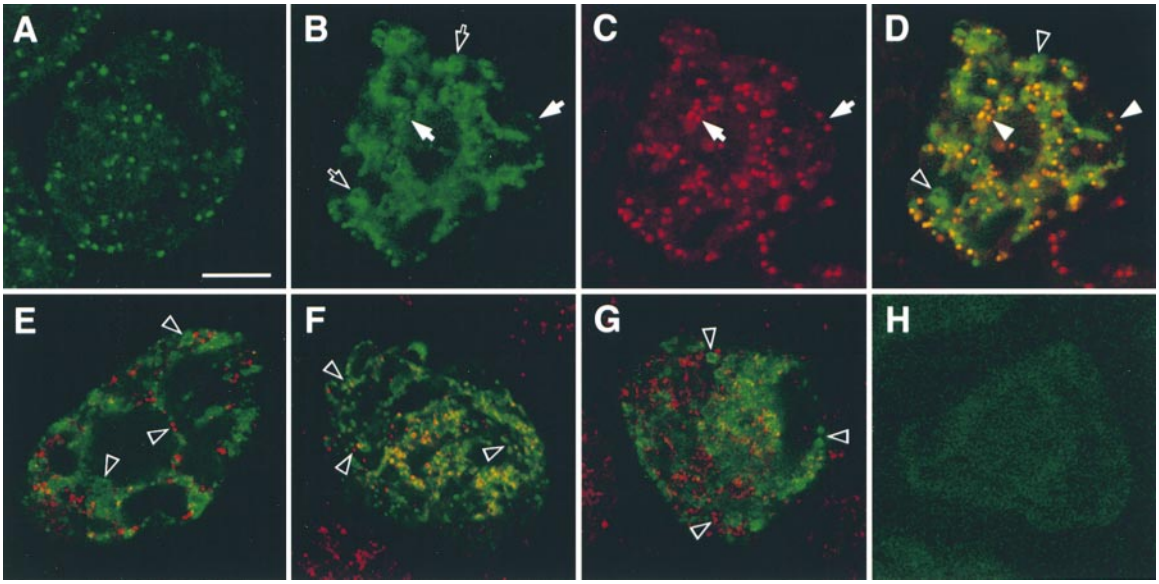

Figure 2. Immunofluorescence Localization of Transiently Expressed HA-pAPX and Endogenous Organelle Marker Proteins in BY-2 Cells.

Nontransformed cells, or cells transiently transformed with HA-pAPX by biolistic bombardment, were fixed in formaldehyde (~20 hr after bombardment), treated with pectolyase Y-23, incubated in 0.3% Triton X-100 (to permeabilize all cellular membranes), and then incubated with primary and dye-conjugated secondary antibodies.

(A) Nontransformed cells exhibiting a punctate Cy2 fluorescence attributable to endogenous peroxisomal APX after application of anti-cucumber peroxisomal APX IgGs.

(B) to **(D)** HA-pAPX–transformed cell showing the colocalization **(D)** of only a portion of expressed HA-pAPX **(B)** with endogenous peroxisomal catalase **(C)**. In **(B)**, both a punctate Cy2 fluorescence (solid arrows) and reticular/circular Cy2 fluorescence (outlined arrows) of HA-pAPX (anti-HA IgGs) are apparent. In **(C)**, only a punctate Cy5 fluorescence (solid arrows) attributed to endogenous catalase (anti-cottonseed catalase IgGs) in peroxisomes is apparent. The merged image in **(D)** shows that the green punctate HA-pAPX fluorescence, but not the reticular/circular fluorescence, colocalizes (yellow/orange) with the red punctate fluorescence of endogenous catalase. Solid arrowheads indicate obvious colocalizations; outlined arrowheads indicate non-colocalizations.

(E) to **(G)** HA-pAPX–transformed cells illustrating the absence of colocalization of expressed HA-pAPX with resident Golgi body (reversibly glycosylated polypeptide) **(E)**, mitochondrial (β-ATPase) **(F)**, and vacuolar (δ isoform of tonoplast intrinsic protein) **(G)** proteins. Outlined arrowheads indicate obvious non-colocalizations between green reticular/circular structures of HA-pAPX and the red organelle markers. Juxtaposition of the HA-pAPX–labeled reticulum (green) and the mitochondria (red) sometimes results in a misleading appearance of yellow/orange colocalization.

(H) Nontransformed cell showing absence of Cy2 fluorescence when primary IgGs are omitted.

Bar in **(A)** = 10 μm for **(A)** to **(H)**.

effects of physical and chemical handling of cells involved in the biolistic bombardment procedure, we also stained living, unbombarded cells with $DiOC_6$. Figure 3E illustrates that a reticular/circular fluorescence pattern similar to that observed in HA-pAPX–transformed (cf. Figure 3B) and in nontransformed neighboring (cf. Figure 3D) cells occurs in normal, living BY-2 cells. The control experiments thus confirm that the reticular/circular network observed with anti-HA antibodies and $DiOC_6$ staining in transformed cells is not a consequence of transient overexpression (or fixation with formaldehyde) of HA-pAPX.

Evidence to help support or refute our interpretation that HA-pAPX was localized to the ER, or to a portion thereof, was sought with antibodies to calreticulin, calnexin, and the lumenal binding protein (BiP), three proteins well-established as resident in the ER. Although we expected that the reticular/circular staining pattern of HA-pAPX would coincide with one or more of the three ER marker proteins, the results were surprisingly different. Figure 3F shows a HA-pAPX reticular/circular immunofluorescence image, and Figure 3G shows in the same cell the immunofluorescence image of calreticulin. As seen in the merged image (Figure 3H), the two antigens are not colocalized. Close inspection of the yellow/orange coloration revealed it to be the vivid fluorescence of juxtaposed antigens rather than true colocalization. A similar three-image comparison for a transformed cell double labeled for HA-pAPX (Figure 3I) and BiP (Figure 3J) is shown as a merged image in Figure 3K. Again, close observation reveals that essentially no colocalization is apparent for these two antigens. Finally, Figure 3L shows only the

merged image for the double-labeling experiments with anti-calnexin and anti-HA IgGs; colocalization is not apparent. One interpretation of these results, for which supporting experimental evidence is presented (see below), is that HA-pAPX is localized to the ER, but primarily in a distinct domain of the ER that does not possess the majority of the resident calreticulin, calnexin, or BiP. Alternatively, the data presented so far could be interpreted to indicate that the HA-pAPX is localized to an unidentified, $DiOC_6$-staining compartment that seems to be closely associated with the ER.

The C Terminus of Peroxisomal APX Sorts Chloramphenicol Acetyltransferase to Peroxisomes and to the Reticular/Circular Network

Chloramphenicol acetyltransferase (CAT) was shown in previous targeting studies to be a suitable passenger protein for appended polypeptides (e.g., Mullen et al., 1997a). Figure 4A shows that transiently expressed CAT accumulates throughout the cytosol. However, when the 36 C-terminal residues of peroxisomal APX, including the single transmembrane domain (Figure 1), were appended to the C terminus of CAT, the fusion protein (CAT-pAPX) was sorted from the cytosol to at least two distinct subcellular sites. Figure 4B shows that after 20 hr of expression, CAT-pAPX localized to both globular and reticular/circular structures within the same cell; in contrast, endogenous catalase within this cell was located only in the globular structures (Figure 4C). In the merged image (Figure 4D), some of the CAT-pAPX colocalized (yellow color) with the endogenous catalase in the globular structures. Similar results were obtained with isocitrate lyase, another endogenous peroxisomal enzyme that was observed only in the globular structures (data not shown). All CAT-pAPX–transformed cells possessed an altered endogenous catalase fluorescence; that is, approximately one to 12 globular catalase-containing structures were observed per cell. Aggregated (enlarged) peroxisomes also were observed in a small percentage (~15%) of HA-pAPX–transformed cells; in both cases, the aggregation appeared to result from "zippering" of the organelle boundary membranes, a consequence of the oligomerization of cytosolic-facing, membrane-bound subunit proteins. Space and focus do not allow inclusion of further details or evidence in this article; they will be presented elsewhere.

Experimental results illustrated in Figures 4E to 4G show that the C terminus (36 amino acid residues) of peroxisomal APX also directs CAT to a portion of the $DiOC_6$-stained compartment (putative ER subdomain). The CAT-pAPX localizated in the reticular/circular network (Figure 4E) also colocalized with a portion of the $DiOC_6$ fluorescence (Figure 4F), as shown by the yellow/orange color in Figure 4G (merged image). These results are essentially the same as those in Figure 3C, that is, partial colocalization of HA-pAPX with $DiOC_6$-fluorescent structures. Also, as was found for HA-pAPX (Figures 3F to 3L), the CAT-pAPX reticular staining pattern did not colocalize with the immunofluorescence attributable to calreticulin, BiP, or calnexin (data not shown). Figure 4H is a representative image of a control experiment in which anti-CAT IgGs were omitted but secondary IgGs conjugated to Cy2 were added. Together, these results indicate that the C-terminal extension of peroxisomal APX contains sufficient topogenic information for sorting CAT to peroxisomes and to a putative subdomain of the ER.

Brefeldin A Interferes with the Sorting of CAT-pAPX and CAT-SKL to Peroxisomes

To elucidate some of the dynamics of the sorting pathway for peroxisomal APX within BY-2 cells, we examined the subcellular location of CAT-pAPX microscopically in cells treated with the fungal toxin brefeldin A (BFA). BFA, among other cellular effects, blocks protein export from the ER by preventing the formation of ER-derived coated vesicles (Klausner et al., 1992; Satiat-Jeunemaitre et al., 1996; Staehelin and Driouich, 1997). We selected CAT-pAPX, rather than HA-pAPX, for this series of experiments because observations of CAT-pAPX in peroxisomal aggregates would be convincing evidence that CAT-pAPX localized to preexisting peroxisomes. If transiently expressed CAT-pAPX were sorted indirectly to preexisting peroxisomes by way of a putative ER subdomain, then incubation of transformed cells in BFA during the postbombardment sorting period should interfere with sorting to these peroxisomes. Alternatively, if CAT-pAPX were sorted concurrently to peroxisomes and the putative ER subdomain, then BFA treatment should not affect sorting to either of these compartments.

Figure 5A illustrates a reticular network attributable to CAT-pAPX localization in a transformed cell maintained 8 to 10 hr after bombardment in BFA. The punctate rhodamine fluorescence shown in Figure 5B illustrates the localization of endogenous catalase in the same cell. Fluorescent globular structures (aggregated peroxisomes) were not observed. The failure of CAT-pAPX to colocalize (Figure 5A) with endogenous catalase (Figure 5B) and the absence of globular (aggregated) peroxisomes revealed that CAT-pAPX was not sorted to preexisting peroxisomes in these BFA-treated cells.

The representative images shown in Figures 5C and 5D illustrate that CAT-pAPX–transformed cells could recover from BFA treatment. Bombarded cells were incubated in BFA for 8 to 10 hr as described above, washed several times, and then incubated in transformation medium minus BFA for an additional 8 to 10 hr. Figure 5C shows that CAT-pAPX was sorted to peroxisomal aggregates and to the reticular/circular network (putative ER subdomain). Endogenous catalase in the same cell (Figure 5D) was localized to peroxisomal aggregates that colocalized with CAT-pAPX (cf. Figures 5C and 5D). Because the endogenous catalase in neighboring nontransformed cells (Figure 5D) was localized

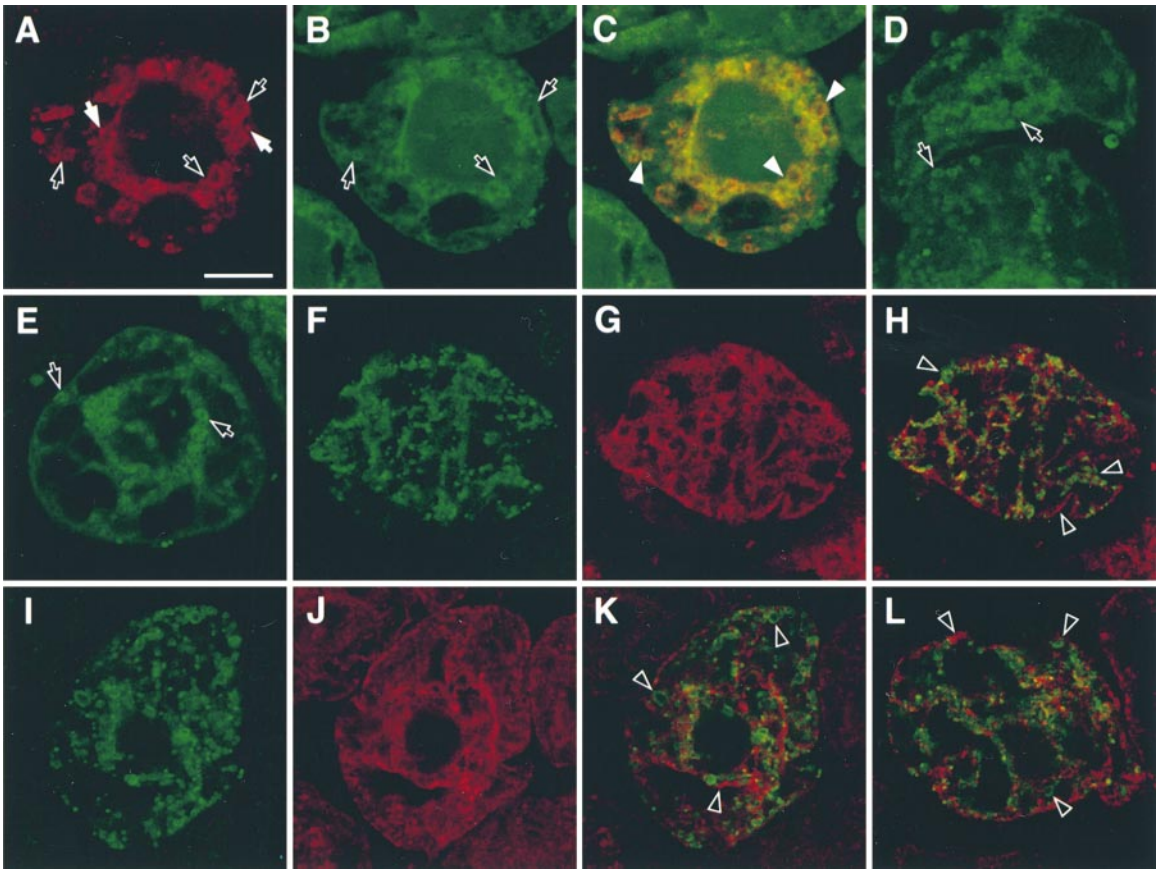

Figure 3. $DiOC_6$ Staining and Immunofluorescence Labeling of ER in BY-2 Cells.

Cells transiently transformed with HA-pAPX (except **[D]** and **[E]**) were fixed (except **[E]**) in formaldehyde (~20 hr after bombardment), treated with pectolyase Y-23, incubated in 0.3% Triton X-100, and then incubated with primary and dye-conjugated secondary antibodies. Cells shown in **(A)** to **(E)** were stained with $DiOC_6$.

(A) to **(C)** HA-pAPX–transformed cell showing the colocalization **(C)** of reticular/circular HA-pAPX **(A)** with a portion of $DiOC_6$-stained membranes (ER) **(B)**. In **(A)**, both the punctate Cy5 fluorescence (solid arrows) and reticular/circular Cy5 fluorescence (outlined arrows) of expressed HA-pAPX (anti-HA IgGs) are apparent. **(B)** shows reticular structures (outlined arrows) attributable to $DiOC_6$ staining in the transformed cell; punctate staining of peroxisomes, indicated by solid arrows in **(A)**, is not apparent. The merged image in **(C)** shows the red reticular/circular HA-pAPX fluorescence, but not the punctate fluorescence (individual peroxisomes), colocalizing (yellow/orange) with a portion of the green reticular $DiOC_6$ fluorescence in the transformed cell. Solid arrowheads indicate obvious colocalizations.

(D) and **(E)** $DiOC_6$ fluorescence in nontransformed cells. Both bombarded (**[D]**, two adjacent cells) and living **(E)** nontransformed cells contain reticular/circular structures (outlined arrows).

(F) to **(H)** HA-pAPX–transformed cell showing the absence of colocalization **(H)** of expressed HA-pAPX **(F)** with endogenous calreticulin **(G)**. The merged image in **(H)** shows that the green reticular/circular Cy2 fluorescence of HA-pAPX does not colocalize with the red reticular Cy5 fluorescence of endogenous calreticulin (anti-castor calreticulin antiserum). Outlined arrowheads indicate obvious structures at which the proteins did not colocalize.

(I) to **(K)** HA-pAPX–transformed cell showing the absence of colocalization **(K)** of expressed HA-pAPX **(I)** with endogenous BiP **(J)**. The merged image in **(K)** shows that the green reticular/circular Cy2 fluorescence of HA-pAPX does not colocalize with the red reticular Cy5 fluorescence of endogenous BiP (anti-maize BiP antiserum). Outlined arrowheads indicate obvious non-colocalizations.

(L) Merged image showing the non-colocalization of expressed HA-pAPX (green) with endogenous calnexin (red, anti-castor calnexin antiserum). Outlined arrowheads indicate obvious non-colocalizations. Faint yellow coloration in **(H)**, **(K)**, and **(L)** is the result of juxtaposition of red and green fluorescent structures.

Bar in **(A)** = 10 μm for **(A)** to **(L)**.

within individual, or "unzippered," preexisting peroxisomes, the peroxisomal aggregation did not result from withdrawal of the BFA. We are therefore confident that the peroxisomal aggregation observed in transformed cells is a consequence of CAT-pAPX sorting to preexisting peroxisomes after removal of BFA. Figure 5E is a representative image from a control experiment illustrating that DMSO, which was included in the BFA solution, does not prevent sorting of CAT-pAPX to peroxisomes (aggregates) or to the putative ER subdomain (reticular/circular structures).

In a positive control experiment, BFA surprisingly also interfered with the sorting of a CAT fusion protein that had a prototypic type 1 PTS, Ser-Lys-Leu, appended to its C terminus (CAT-SKL). At 8 to 10 hr after bombardment in the absence of BFA, CAT-SKL was localized almost exclusively to individual peroxisomes, as expected (Figure 5F). In the presence of BFA, however, CAT-SKL accumulated throughout the cytosol, being only partially localized to individual peroxisomes (Figure 5G). This apparently was not a result of temporal expression because similar images were observed when CAT-SKL was expressed transiently for 20 hr in BFA (data not shown).

To evaluate the possible nonspecific interference of BFA on post-translational sorting of proteins to organelles, we examined as a control the targeting of a CAT fusion protein to mitochondria in the presence of BFA. Chaumont et al. (1994) have shown previously that the 60–amino acid presequence on the tobacco mitochondrial F_1-ATPase β subunit

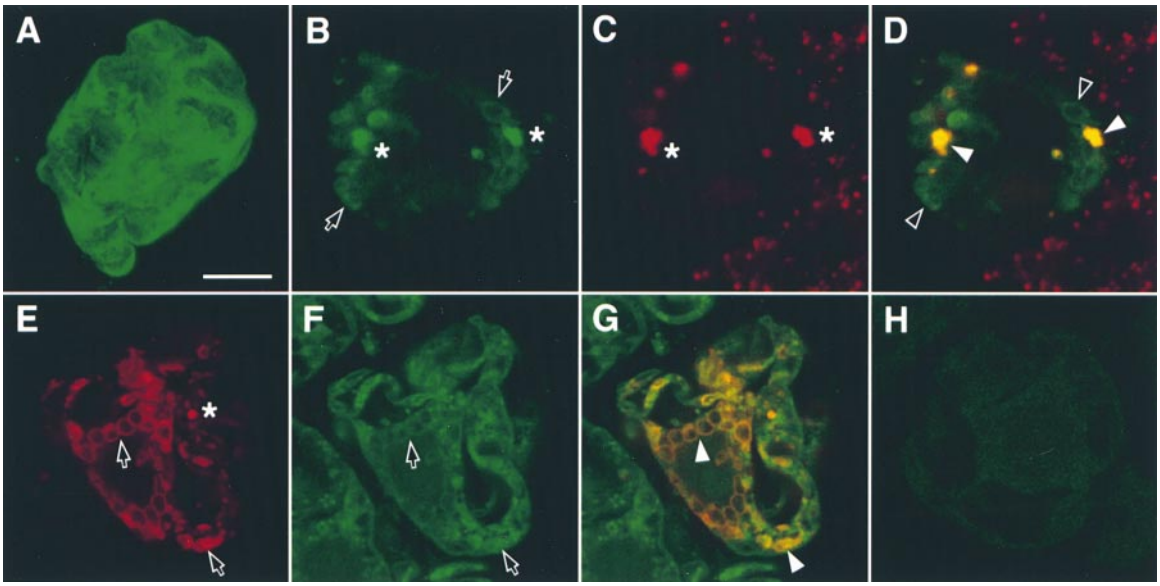

Figure 4. Immunofluorescence Images Illustrating Sorting of CAT-pAPX to Preexisting Peroxisomes and Reticular/Circular Structures.

Transiently transformed cells were fixed in formaldehyde (~20 hr after bombardment), treated with pectolyase Y-23, incubated in 0.3% Triton X-100, and then incubated with primary and dye-conjugated secondary antibodies. In **(E)** to **(G)**, cells also were incubated in $DiOC_6$. **(A)** shows a composite image (projection) of multiple optical sections.

(A) CAT-transformed cell exhibiting Cy2 fluorescence throughout the cytosol (anti-CAT IgGs).

(B) to **(D)** CAT-pAPX–transformed cell showing the colocalization **(D)** of a portion of expressed CAT-pAPX **(B)** with endogenous peroxisomal catalase **(C)**. In **(B)**, both globular Cy2 fluorescence (asterisks) and reticular/circular Cy2 fluorescence (outlined arrows) of CAT-pAPX (anti-CAT IgGs) are apparent. In **(C)**, nearly all Cy5 fluorescence attributed to endogenous catalase (anti-cottonseed catalase IgGs) is globular (asterisks). The merged image in **(D)** shows that the green globular CAT-pAPX fluorescence, but not the reticular/circular fluorescence, colocalizes (yellow/orange) with the red globular fluorescence of endogenous catalase in aggregated (enlarged) peroxisomes. Solid arrowheads indicate obvious colocalizations; outlined arrowheads indicate non-colocalizations.

(E) to **(G)** CAT-pAPX–transformed cell showing the colocalization **(G)** of reticular/circular CAT-pAPX **(E)** with a portion of $DiOC_6$-stained membranes (ER) **(F)**. In **(E)**, both a globular Cy5 fluorescence (asterisk) and reticular/circular Cy5 fluorescence (outlined arrows) of CAT-pAPX are apparent. **(F)** shows a reticular fluorescence pattern (outlined arrows) attributable to $DiOC_6$ staining in the transformed (and surrounding nontransformed) cell. The merged image in **(G)** shows that the red reticular/circular CAT-pAPX fluorescence, but not the globular fluorescence (aggregated peroxisomes), colocalizes (yellow/orange) with a portion of the green reticular $DiOC_6$ fluorescence. Solid arrowheads indicate obvious colocalizations.

(H) Representative image illustrating lack of fluorescence in a CAT-pAPX–transformed cell after application of Cy2-conjugated anti-mouse IgGs only (anti-CAT IgGs were omitted).

Bar in **(A)** = 10 μm for **(A)** to **(H)**.

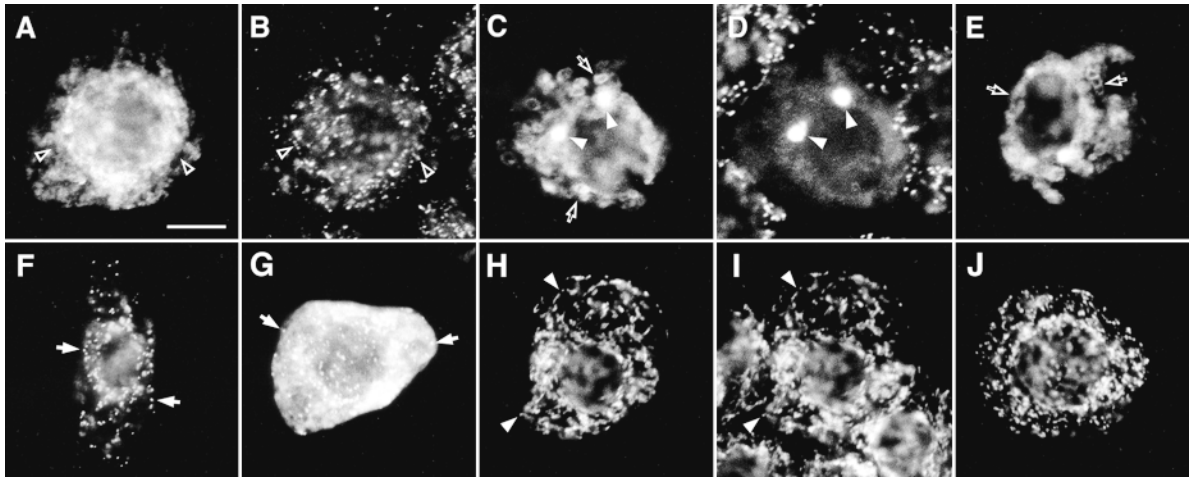

Figure 5. Epifluorescence Images Illustrating the Interference of BFA with the Sorting of CAT-pAPX to BY-2 Peroxisomes.

Cells were biolistically bombarded in transformation medium with or without 100 μg/mL BFA. After transient expression for 8 to 10 hr, cells were fixed in formaldehyde, treated with pectoylase Y-23, incubated in 0.3% Triton X-100, then incubated with primary and dye-conjugated secondary antibodies. For the recovery experiments in **(C)** and **(D)**, bombarded cells were incubated in transformation medium plus BFA for 8 to 10 hr and then washed and incubated in transformation medium without BFA for an additional 8 to 10 hr. In **(E)**, only DMSO (no BFA) was added to the transformation medium. In **(F)** to **(J)**, CAT-SKL and CATβ60 were expressed for 8 to 10 hr prior to fixation.

(A) and **(B)** CAT-pAPX–transformed cell (treated with BFA) exhibiting a reticular Cy2 fluorescence attributable to overexpressed CAT-pAPX (anti-CAT IgGs) **(A)** and a punctate rhodamine fluorescence attributable to endogenous catalase (anti-cottonseed catalase IgGs) that is not colocalized in individual peroxisomes (outlined arrowheads) **(B)**.

(C) and **(D)** CAT-pAPX–transformed cell (no BFA) showing the colocalization (solid arrowheads) of a portion of expressed CAT-pAPX **(C)** with endogenous catalase **(D)** in globular peroxisomes. In **(C)**, both globular and reticular/circular structures (outlined arrows) exhibit Cy2 fluorescence from CAT-pAPX. In **(D)**, all rhodamine fluorescence attributable to endogenous catalase is globular.

(E) CAT-pAPX–transformed cell, bombarded in transformation medium containing 1% (v/v) DMSO, exhibiting reticular/circular (outlined arrows) and globular Cy2 fluorescence.

(F) CAT-SKL–transformed cell (no BFA) exhibiting a punctate Cy2 fluorescence (solid arrows) attributable to CAT-SKL localized in individual peroxisomes.

(G) CAT-SKL–transformed cell (treated with BFA) exhibiting cytosolic and punctate (solid arrows) Cy2 fluorescence attributable to CAT-SKL localized in the cytosol and in individual peroxisomes, respectively.

(H) and **(I)** CATβ60-transformed cell (no BFA) showing the colocalization (solid arrowheads) of punctate Cy2 fluorescence attributable to expressed CATβ60 **(H)** with the punctate Cy3 fluorescence attributable to endogenous mitochondrial β-ATPase E **(I)**.

(J) CATβ60-transformed cell (treated with BFA) exhibiting a punctate Cy2 fluorescence pattern attributable to CATβ60 localized to mitochondria. Bar in **(A)** = 10 μm for **(A)** to **(J)**.

is sufficient to target CAT to mitochondria in transgenic tobacco. Figure 5H illustrates that at 8 to 10 hr after bombardment the CAT fusion protein (CATβ60) had sorted in transformed cells to mitochondria, which were observed as numerous rod-shaped immunofluorescent structures. These CATβ60-containing structures colocalized with the rod-like immunofluorescence in the same cells that could be attributed to endogenous mitochondrial β-ATPase E (Figure 5I). Figure 5J shows that when CATβ60-bombarded cells were maintained in BFA for ~9 hr, the CAT fusion protein was targeted to mitochondria in a normal fashion. Thus, the results presented in Figures 5A to 5J indicate that BFA interferes with the post-translational sorting of proteins to the boundary membrane and matrix of peroxisomes but not with the sorting of a protein to the matrix of mitochondria.

Peroxisomal APX Is Inserted Post-Translationally into ER Membranes in Vitro

In vitro membrane insertion/association experiments were performed to help interpret results of the in vivo microscopic sorting experiments. To properly test our working hypothesis that proteins were sorted indirectly to peroxisomes by way of the ER, it was particularly important to use highly purified ER membranes in the in vitro assays. Table 1 shows that these microsomal-derived ER membranes (MEMs) fit this criterion. The microsomal fraction (the pellet obtained after ultracentrifugation at 100,000*g* for 60 min) was enriched with the two functionally independent ER markers UDP–GlcNAc transferase and NADH–cytochrome *c* reductase. As shown by the presence of various enzymes, it also

contained significant amounts of mitochondrial (succinate dehydrogenase), peroxisomal (catalase), and plastidic (ribulose bisphosphate carboxylase oxygenase) proteins, with some Golgi body (acid phosphatase) proteins. Equilibrium density sucrose gradient centrifugation of these microsomes, followed by gel permeation chromatography of the ER band from this gradient, yielded highly purified MEMs that possessed some mitochondria and considerably less peroxisomal contamination (Table 1).

For most of the experiments we used a coupled transcription/translation rabbit reticulocyte lysate system programmed with DNA coding for cottonseed peroxisomal APX (Figures 6A and 6B). Lane 1 (Figure 6A) shows that a single product of the expected molecular mass for the peroxisomal APX polypeptide (31 kD) was recovered in the soluble fraction of the reticulocyte lysate. Lane 2 illustrates that when MEMs were added 1 hr after initiation of the transcription/translation reactions, a 31-kD product (constituting 94% of the total radiolabeled pAPX, as determined by radioanalytical imaging) was in the membrane pellet collected after centrifugation through a sucrose cushion. Resuspension of these membranes in 100 mM sodium carbonate, pH 11.5, and recentrifugation through an alkaline sucrose cushion resulted in recovery of all (116%) of the peroxisomal APX in the pellet fraction (lane 3), indicating that peroxisomal APX was integrated stably into the MEMs. Washing an MEM preparation with 300 mM KCl (to remove signal recognition particles) before adding it to the translation mixture did not inhibit integration of peroxisomal APX into membranes (lane 4), the measured value being 107% that of the unwashed sample. Collectively, these data indicate that peroxisomal APX integrates in vitro into ER membranes in a post-translational (signal recognition particle–independent) manner.

Removal of ATP from translation mixtures by the addition of apyrase greatly reduced (90%) the post-translational insertion of peroxisomal APX into MEMs (Figure 6A, cf. lanes 5 and 3). Pretreatment of MEMs with trypsin also substantially reduced (97%) membrane insertion of peroxisomal APX (Figure 6A, cf. lanes 6 and 3), indicating that a protease-sensitive membrane component is required for peroxisomal APX insertion. Intact peroxisomal APX remained in the supernatant after treatment with alkaline sodium carbonate (data not shown), indicating that residual protease did not digest peroxisomal APX and thus gave results different from those shown in lane 6. Figure 6A, lane 7, shows that membrane-inserted peroxisomal APX, obtained in experiments described for lane 3, was digested by trypsin afterwards, indicating that most of the polypeptide chain faces outward on membrane vesicles. This is consistent with the topological orientation of peroxisomal APX determined by us in in vivo experiments and by others for peroxisomes in other cell types (Yamaguchi et al., 1995; Ishikawa et al., 1998).

Results presented in Figure 6B show that peroxisomal APX integrates specifically into MEMs (93%; lane 5) and not into membranes of mitochondria (0%; lane 1), chloroplasts (0%; lane 2), or plasma membranes (0%; lane 3). Relatively little peroxisomal APX integrated into peroxisomal membranes (5%; lane 4). Data on the purity of these membranes have been published elsewhere (see Methods). When in vitro reaction mixtures were programmed with the DNA encoding HA-pAPX, virtually the same results were obtained as with peroxisomal APX DNA: HA-pAPX was integrated efficiently into MEMs (85%; lane 7) but not into peroxisomal membranes (2%; lane 6). Positive controls (lanes 8 to 11) show that *S. cerevisiae* Pex15p (Elgersma et al., 1997) and mouse synaptobrevin/vesicle-associated membrane protein 2

Table 1. Distribution and Percentage of Recoveries of Marker Enzyme Activities and Rubisco Protein in Subcellular Fractions Prepared from Cultured Maize Endosperm Cells

	Fraction[b]		
Enzyme[a]	Homogenate	100,000*g* Pellet	MEM
Alcohol dehydrogenase (ADH)	16.8 ± 0.14 (100)	0.11 ± 0.09 (0.6)	0 (0)
Succinate dehydrogenase (SDH)	0.88 ± 0.06 (100)	0.14 ± 0.07 (15.9)	0.08 ± 0.01 (9.1)
Catalase	25.29 ± 2.22 (100)	7.72 ± 0.61 (30.5)	0.82 ± 0.12 (3.2)
Rubisco protein	100 (100)	6.6 ± 1.0 (6.6)	0 (0)
Acid phosphatase	73.0 ± 3.2 (100)	1.8 ± 0.6 (2.5)	0.22 ± 0.02 (0.3)
UDP–GlcNAc transferase	2.1 ± 0.13 (100)	1.7 ± 0.09 (81.0)	1.36 ± 0.09 (64.8)
NADH–cytochrome *c* reductase	24.2 ± 2.2 (100)	17.1 ± 1.4 (71.0)	15.1 ± 1.2 (62.0)

[a] Enzyme units: ADH, μmol min^{-1}; SDH, μmol hr^{-1}; catalase, Lück units × 10^{-3}; ribulose bisphosphate carboxylase oxygenase (Rubisco) protein, arbitrary units as determined by ELISA; acid phosphatase, μmol min^{-1}; UDP–GlcNAc transferase, μmol hr^{-1}; NADH–cytochrome *c* reductase, pmol hr^{-1}.

[b] Numbers in parentheses are the percentage of recoveries. Total recoveries among fractions derived from homogenates were as follows: ADH, 100%; SDH, 94%; catalase, 92%; Rubisco, 109%; acid phosphatase, 138%; UDP–GlcNAc transferase, 92%; NADH–cytochrome *c* reductase, 104%. Data presented are mean ±SE for the seven different preparations used in this paper.

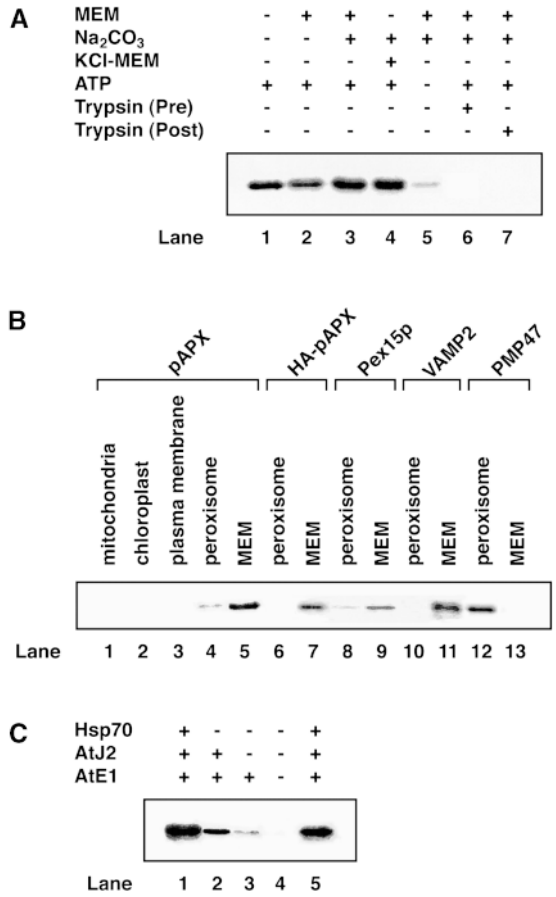

Figure 6. Insertion of Peroxisomal APX into ER Membranes in Vitro.

For data shown in **(A)** to **(C)**, radiolabeled proteins were acid precipitated, separated by SDS-PAGE in 12.5% acrylamide gels, and visualized with an AMBIS radioanalytical imaging system.

(A) pAPX integrates post-translationally into ER membranes. Lane 1 contains radiolabeled peroxisomal APX that was synthesized for 1 hr at 25°C from a cDNA in a coupled in vitro transcription/translation assay in the presence of ^{35}S-methionine; lane 2, translation reactions (terminated after 1 hr by the addition of emetine) were incubated with MEMs for 1 hr at 25°C, after which membranes were collected by centrifugation through a sucrose cushion; lane 3, the MEM pellet described for lane 2 was resuspended and extracted with 100 mM Na_2CO_3, pH 11.5, to remove soluble and peripheral membrane-associated proteins from the remaining integral membrane proteins, and the MEMs were repelleted by centrifugation through an alkaline sucrose cushion; lane 4, same as lane 2 except that MEMs were prewashed in 300 mM KCl to remove membrane-bound ribosomes (including signal recognition particles); lane 5, same as lane 2, except that the completed translation reactions were preincubated with apyrase for 30 min at 25°C to remove ATP; lane 6, MEMs were pretreated with trypsin at 4°C for 30 min before incubation with translation reactions and later were extracted in Na_2CO_3 as described for lane 3; and lane 7, MEM translation reaction mixtures were incubated with trypsin at 4°C for 30 min and then extracted in Na_2CO_3 as described for lane 3. Addition to the reaction mixtures is indicated as (+), omission as (−).

(B) Comparison of the insertion of peroxisomal APX and other membrane proteins into various organelle membranes. Peroxisomal APX (lanes 1 to 5), HA-pAPX (lanes 6 and 7), *S. cerevisiae* Pex15p (lanes 8 and 9), mouse VAMP2 (lanes 10 and 11), and the 47-kD peroxisomal membrane protein PMP47 from *C. boidinii* (lanes 12 and 13) were synthesized from their corresponding cDNAs by using a coupled in vitro transcription/translation system in the presence of ^{35}S-methionine. Various membrane vesicles (as indicated above lanes) were incubated in terminated reaction mixtures for 1 hr at 25°C. Membranes were collected by centrifugation through a sucrose cushion, resuspended in 100 mM Na_2CO_3, and recentrifuged through an alkaline sucrose cushion.

(C) Inhibition of peroxisomal APX integration into ER membranes by immunodepletion of molecular chaperones from translation mixtures. Peroxisomal APX RNA was translated in vitro by using a wheat germ–derived translation system (lane 1). Wheat germ extracts were incubated with antibodies before the translation reactions, and MEMs were added after translation for 1 hr at 25°C. The following antibodies were added to pre-translation reactions: anti-Hsp70 antibodies (lane 2); anti-Hsp70 plus anti-AtJ2 antibodies (lane 3); anti-Hsp70, anti-AtJ2, and anti-AtE1 antibodies (lane 4); anti-pyruvate dehydrogenase E1α subunit antibodies (lane 5). MEMs were collected by centrifugation through a sucrose cushion, resuspended in 100 mM Na_2CO_3, and recentrifuged through an alkaline sucrose cushion. Addition to the reaction mixtures is indicated as (+), omission as (−).

(VAMP2) (Weber et al., 1998) also were integrated into ER membranes (43% and 94%, respectively) but were not efficiently integrated into peroxisomal membranes (5% and 3%, respectively), as expected. In contrast, PMP47 from *C. boidinii* (McCammon et al., 1994) inserted into peroxisomal membranes (66%; lane 12) but not into ER membranes (5%; lane 13), also as anticipated.

A wheat germ system programmed with peroxisomal APX RNA was used to assess the results of immunodepleting molecular chaperones from the translation mixtures (Figure 6C). Comparing lanes 1 and 2 shows that immunodepletion of the 70-kD heat shock chaperone protein (Hsp70) (Miernyk et al., 1992) resulted in inefficient (32%) insertion into ER membranes. Lanes 3 and 4 show that immunodepletion of Hsp70 plus the chaperone AtJ2, a homolog of *Escherichia coli* DnaJ (Zhou et al., 1995) (lane 3), or immunodepletion of Hsp70, AtJ2, and the nucleotide exchange factor AtE1, a functional homolog of *E. coli* GrpE (B. Kroczynska and J.A. Miernyk, unpublished data) (lane 4), resulted in little (9%) or no (0%) detectable insertion of peroxisomal APX into ER membranes, respectively. Lane 5 shows results of a control reaction in which peroxisomal APX insertion (94%) into MEMs was relatively unaffected when wheat germ extracts were incubated with the unrelated anti-pyruvate dehydrogenase E1α subunit antibody. These results indicate that the Hsp70 reaction cycle, or the recently renamed Hsp70 chaperone machine (Bukau and Horwich, 1998), is involved in the insertion of peroxisomal APX into ER membranes in vitro.

DISCUSSION

We used two approaches to elucidate the intracellular sorting of cottonseed peroxisomal APX to its functional site in the peroxisome boundary membrane. Immunofluorescence microscopy of gene products transiently expressed in BY-2 cells provided novel in vivo subcellular localization information, and results from in vitro protein association/insertion assays complemented those from the microscopic analyses. In BY-2 cells, HA-epitope–tagged peroxisomal APX localized to two distinct subcellular sites, peroxisomes and a reticular/circular network, the latter postulated to be a distinct subdomain of the ER. Results from in vitro experiments also showed that peroxisomal APX was inserted directly into purified ER membranes, but not into peroxisomal membranes, in a post-translational manner that depended on the presence of ATP and molecular chaperones. Collectively, our findings support the notion that, as with several mammalian and yeast PMPs, plant peroxisomal APX is sorted to peroxisomes by way of the ER.

Peroxisomal APX Sorts to a Reticular/Circular Compartment in Vivo

As shown by the immunofluorescence data presented here, overexpression of peroxisomal APX in BY-2 cells provides the opportunity to discern and dissect the sorting pathway of this important enzymatic PMP. The localization of expressed HA-pAPX to a nonperoxisomal compartment(s) raised the question as to why endogenous peroxisomal APX was observed only in peroxisomes in normal BY-2 cells (Figure 2A) and in oilseed cotyledons (Corpas et al., 1994; Yamaguchi et al., 1995; Bunkelmann and Trelease, 1996; Ishikawa et al., 1998). Although it seems reasonable that the greatest proportion of peroxisomal APX at its steady state is within the peroxisomal boundary membrane, whereas in overexpressing cells, the protein is detectable throughout its sorting pathway (including the putative ER subdomain), one could also argue that the reticular/circular network was formed as a result of peroxisomal APX overexpression, cell fixation conditions, or both.

Results from several sources, however, indicate that neither of these possibilities is likely. For example, the network is readily observed in living, unbombarded cells stained with $DiOC_6$ (Figure 3E), and similar structures are seen consistently in both nontransformed (Figure 3D) and transformed cells (Figures 3C and 4G) within bombarded samples fixed in formaldehyde and in unbombarded cells fixed in glutaraldehyde (not shown). In other cells, such as moss caulonemata (McCauley and Hepler, 1990) and cultured mammalian Madin–Darby canine kidney cells (Hannan and Edidin, 1996), $DiOC_6$ also labels a reticular/circular network. Furthermore, immunofluorescence localization of calreticulin in mature leaves of maize (Napier et al., 1995) and cotyledons of germinated tobacco seeds (Denecke et al., 1995) has provided morphological evidence that a similar network occurs in plant tissues as well as in cultured cells. Thus, numerous observations and literature examples have convinced us that the reticular/circular network described in this study represents an authentic membranous compartment(s) within BY-2 cells.

Intriguing evidence for the apparent sorting of peroxisomal APX to the ER comes from the colocalization of HA-pAPX (and CAT-pAPX) with a portion of the reticular/circular network that stains with $DiOC_6$ (solid arrowheads in Figures 3C and 4G). As referenced above with specific examples, $DiOC_6$ commonly is used to label ER fluorescently in a variety of fixed and living cells (see also Terasaki, 1993; Sabnis et al., 1997), but it also has been shown to label mitochondria and other organelles. Despite this caveat, we varied the concentration of $DiOC_6$ in preliminary experiments to achieve optimal staining of the ER network. Although some punctate (mitochondrial) fluorescence was observed even under optimized conditions, we discounted this background, given that HA-pAPX did not sort to mitochondria, Golgi, plastids, or vacuoles (Figures 2E to 2G). Thus, the reticular/circular network that could be immunostained in cells expressing HA-pAPX or CAT-pAPX (Figures 2D and 4D) and that colocalized with $DiOC_6$ (Figures 3C and 4G) seems to be morphologically and logically part of the ER. The virtual lack of colocalization of this network with common ER resident proteins (Figures 3H, 3K, and 3L) indicates that if peroxisomal APX is indeed localized to the ER, then a distinct subdomain that somehow is involved in the eventual distribution of PMPs to (preexisting) peroxisomes (discussed below) must exist.

As presented in the Introduction, the sorting of PMPs to peroxisomes by way of the ER is not without precedent in the literature, at least in mammalian and yeast cells. For example, yeast cells expressing either ER-targeted PMPs (Baerends et al., 1996; Elgersma et al., 1997; Kammerer et al., 1998) or ER membrane proteins (Wright et al., 1988; Vergeres et al., 1993) showed a marked elaboration of ER membranes. In particular, Pex15p specifically accumulated in proliferated ER in *S. cerevisiae* cells that were overexpressing this protein (Elgersma et al., 1997). Furthermore, Pex2p and Pex16p were N-glycosylated within the ER lumen while en route to peroxisomes in *Yarrowia lipolytica* mutants that were defective both in protein egress from the ER and in peroxisome biogenesis (Titorenko et al., 1997). Our finding that peroxisomal APX sorts to a compartment that morphologically resembles the ER suggests this organelle may be involved in directing plant PMPs as well.

Peroxisomal APX Is Inserted into Isolated ER Membranes in Vitro

A comprehensive series of in vitro experiments was performed to obtain further evidence for or against involvement of the ER in the post-translational sorting of peroxisomal APX. Well-established procedures were used (Miernyk et al.,

1992), and the purity (Table 1) and uptake competency of the highly purified ER vesicles (MEMs) were exemplary. The membranes from other organelles were prepared from plant species that provide some of the purest membranes that can be prepared from these particular organelles; the species source was not considered a factor in interpreting the data. Three lines of in vitro evidence supported post-translational sorting/insertion of peroxisomal APX to or into the ER: the insertion of peroxisomal APX into MEMs after translation was arrested by the addition of emetine and RNase (our standard protocol); the efficiency of peroxisomal APX insertion was not enhanced when MEMs were added to reaction mixtures during the first hour of translation (data not shown); and the peroxisomal APX was inserted into MEMs in the absence of signal recognition particles (stripped from MEMs with KCl; Figure 6A, lane 4). Additional evidence came from our unpublished time-course studies in vivo. At ~4 to 5 hr after bombardment, at least part of the immunofluorescence attributable to the expressed HA-pAPX was observed in the cytosol and was not associated with reticular/circular or punctate structures. If peroxisomal APX were inserted cotranslationally in vivo, then peroxisomal APX most probably would have been detected only in the ER and/or peroxisomes at all post-bombardment times.

The insertion of PMPs (rat peroxisomal assembly factor-1, PMP22, PMP70, and Arabidopsis PMP22) into peroxisomal membranes in vitro has been reported to be independent of ATP (Imanaka et al., 1996; Just and Diestelkötter, 1996; Tugal et al., 1999). These results seemingly are in contrast to those obtained here for peroxisomal APX; that is, the addition of apyrase to reaction mixtures markedly reduced insertion of peroxisomal APX into MEMs (Figure 6A, lane 5). Considering that importing proteins directly into the peroxisomal matrix also requires ATP (Horng et al., 1995; Olsen, 1998; Subramani, 1998), it may be inappropriate to make comparisons of the ATP-dependent insertion of peroxisomal APX with the ATP-independent insertion of the above-listed PMPs. However, peroxisomal APX is inserted into ER membranes and not into peroxisomal membranes, whereas all of the PMPs listed above were shown previously to have been inserted directly into peroxisomal membranes in vitro.

Molecular chaperones have been implicated in the acquisition of peroxisomal matrix proteins; however, data for interactions with a membrane protein have been reported in only one study. Pause et al. (1997) found that rat PMP22 coimmunoprecipitated separately with two proteins in rabbit reticulocyte lysate mixtures, namely, the chaperonin TRiC and a 40-kD polypeptide of unknown function. Frydman et al. (1994) also reported the apparent involvement of TRiC but only for the import of matrix proteins. Both groups proposed that the TRiC interacted with other chaperones, such as Hsp70, Hsp90, and DnaJ, as reported for uptake of matrix proteins (Walton et al., 1994; Crookes and Olsen, 1998; Hettema et al., 1998).

In our study, apparent interaction with the three components of the Hsp70 chaperone machine (Bukau and Horwich, 1998) substantially influenced insertion of peroxisomal APX into MEMs. Immunodepletion of Hsp70 alone, which is a relatively abundant component in wheat germ extracts (Miernyk et al., 1992), reduced peroxisomal APX insertion by ~70% (Figure 6C, lane 2). Additional immunodepletion of the cytosolic DnaJ homolog and the nucleotide exchange factor, two other members of the Hsp70 machine, cooperatively abolished insertion of peroxisomal APX into MEMs. Whether removal of ATP with apyrase, which resulted in less efficient insertion, affected chaperone function is not known. Nonetheless, the cooperative interactive necessity of all of these components for acquisition of any matrix or membrane protein into peroxisomes or the ER has not been reported previously. Our data, and those related to TRiC interactions, provide substantial evidence that post-translational sorting of peroxisomal APX to the ER (or of other PMPs directly to peroxisomes) involves the cooperative action of cytosolic molecular chaperones and the presence of ATP. This does not preclude subsequent interaction(s) with proteinaceous components in the boundary membranes, such as a putative membrane-bound chaperone (Corpas and Trelease, 1997) or a putative PMP receptor (Ballard et al., 1998; Figure 6A, lane 6).

One realistic concern related to our interpretations of in vitro insertions of membrane proteins was the possibility of nonspecific, hydrophobic interactions between peroxisomal APX and any added target membrane. Such was not the case, however, because nascent peroxisomal APX was consistently inserted at high efficiencies into MEMs but not to any appreciable extent into other added membranes derived from mitochondria, plastids, plasma membranes, or peroxisomes (Figure 6B). An important control was that the peroxisome membranes used in this study were indeed capable of acquiring a PMP in vitro. *C. boidinii* PMP47 inserted specifically into peroxisome membranes but not into MEMs (Figure 6B, lanes 12 and 13), confirming the findings of Dyer et al. (1996), who showed that PMP47 did not sort to ER in vivo but was targeted directly from the cytosol to peroxisomes. Two other experiments performed as positive controls revealed that mouse VAMP2 and *S. cerevisiae* Pex15p were inserted into MEMs and not into peroxisomes, as was predicted from published results (Kutay et al., 1995; Elgersma et al., 1997). These controls add credibility to our contention that newly synthesized peroxisomal APX selectively sorts post-translationally to, and inserts into, the ER in plant cells. We were not able, however, to learn from the in vitro experiments whether peroxisomal APX sorts to a subdomain of ER, as had been postulated from the immunofluorescence studies.

Does Peroxisomal APX Sort to Peroxisomes by Means of ER Transport Vesicles?

Virtually all preexisting peroxisomes become aggregated as CAT-pAPX sorts to these organelles, a phenomenon that

provided an added dimension for interpreting the results of BFA treatments because it enabled us to distinguish between events that involved putative preperoxisomal compartments or preexisting peroxisomes. Detailed results describing the progressive aggregation of CAT-pAPX–bound peroxisomes (apparently by oligomerization of CAT polypeptides on the cytosolic face of these peroxisomes) will be presented in another paper (R.T. Mullen, C.S. Lisenbee, and R.N. Trelease, in preparation).

In BFA-treated cells, the accumulation of CAT-pAPX in the ER (circular/reticular network; Figure 5A) and its absence in preexisting peroxisomes (peroxisomes not aggregated; Figure 5B) are interpreted to result from BFA preventing the formation/exit of vesicles from the ER that ordinarily would sort to preexisting peroxisomes. Supporting evidence for this interpretation was obtained from immunofluorescence images of cells that had been relieved from the effects of BFA. In these cells, CAT-pAPX was observed in aggregated preexisting peroxisomes (Figures 5C and 5D) apparently because the CAT-pAPX was allowed to exit the ER. BFA affects vesicular formation/transport from the ER (Klausner et al., 1992; Staehelin and Driouich, 1997), and BFA treatment in another system has been interpreted to block ER vesicle formation and subsequent transport to preexisting peroxisomes (Salomons et al., 1997); consequently, we suggest that CAT-pAPX exits ER within vesicles.

Two sets of positive controls were performed as part of the BFA experiments, namely, the post-translational targeting of a mitochondrial protein (CATβ60) and a peroxisomal matrix protein (CAT-SKL) in the presence of BFA. The protein destined to insert into mitochondria was acquired by mitochondria without any notable effect of BFA (Figures 5H to 5J). The same result was expected for CAT-SKL because peroxisomal matrix proteins generally are thought to be targeted directly from the cytosol to preexisting peroxisomes (Olsen, 1998; Subramani, 1998). However, our results with the sorting of CAT-SKL, and the results of Salomons et al. (1997) with *H. polymorpha* alcohol oxidase (a peroxisomal matrix enzyme), in BFA-treated cells shed a different light on this widely accepted view. CAT-SKL accumulated mostly in the cytosol (Figure 5G), whereas alcohol oxidase accumulated in the ER.

Salomons et al. (1997) suggested that *H. polymorpha* matrix proteins are delivered to their target organelle together with membrane components by accumulating with PMPs either in the ER or in transport vesicles that migrate to preexisting peroxisomes. In BY-2 cells, the mostly cytosolic localization of CAT-SKL seems to be a strong indication that CAT-SKL (representing most or all of the matrix-destined proteins with a PTS1) is not sorted directly to peroxisomes or to the ER. Why is some of the CAT-SKL located in peroxisomes (Figure 5G)? An explanation similar to one given for alcohol oxidase sorting in *H. polymorpha* (Salomons et al., 1997) is that CAT-SKL normally sorts to ER-derived transport vesicles and that some of the expressed CAT-SKL was sorted to such vesicles that had formed before uptake of BFA. Or, perhaps CAT-SKL accumulated in the cytosol as an indirect consequence of the failure to assemble membrane-bound components of the translocation machinery. Of course, some matrix proteins may sort directly to preexisting peroxisomes.

Salomons et al. (1997) further speculated that in yeast cells, only a subset of PMPs, that is, "functional" membrane proteins such as transporters (e.g., PMP47) and presumably enzymes (e.g., peroxisomal APX), sorts directly from the cytosol to preexisting peroxisomes. In contrast, they suggested that PMPs involved in early stages of peroxisome biogenesis, that is, "early peroxins" such as Pex15p, sort indirectly to peroxisomes by way of the ER and ER-derived vesicles. Kunau and Erdmann (1998) make similar predictions for these types of proteins. Our in vitro data support the postulates for Pex15p and PMP47 (Figure 6B, lanes 8 and 9, and 12 and 13) but not for peroxisomal APX (Figure 6B, lanes 6 and 7). Thus, there appear to be various pathways for sorting PMPs, but at this early stage of investigation, our data do not support the generalization that is emerging from studies of yeast peroxisomal biogenesis that "functional" PMPs sort through a different pathway from that involving "biogenesis" PMPs.

Overview of a Sorting Pathway through a Putative Peroxisomal ER Subdomainm

The ER is a dynamic membranous compartment, constituted functionally as an assemblage of specialized regions or subdomains (Hepler et al., 1990; Sitia and Meldolesi, 1992; Okita and Rogers, 1996; Staehelin, 1997). The distinct ER subdomain that seems to be involved in the sorting of peroxisomal APX to BY-2 peroxisomes is distinguishable as a portion of the reticular/circular ER to which HA-pAPX is localized and reticuloplasmins somehow are not (Figures 3H, 3K, and 3L). Reticuloplasmins (e.g., BiP, calnexin, and calreticulin) are believed to exist within the same subdomain of the ER (Crofts and Denecke, 1998), although they (and their subdomains?) are not necessarily distributed uniformly throughout the ER (Okita and Rogers, 1996). Clearly, much needs to be learned about the localizations of resident and cargo proteins within the ER. Our non-colocalization results for peroxisomal APX and the reticuloplasmins are consistent with current generalizations that include spatial and functional separations of these proteins.

The "privileged site budding model" (Kuehn and Schekman, 1997) and modifications thereof (Aridor et al., 1998; Hobman et al., 1998) seem to offer a reasonable working explanation for the lack of colocalization of HA-pAPX and reticuloplasmins and for the putative vesicular exit of PMPs from specific subdomains of the ER. In general, the models suggest that cargo proteins sequestered within the lumen or membrane of the ER are concentrated within specific subdomains or "privileged sites" before export by COPII vesicles. "Gating proteins" are postulated to allow cargo to enter the privileged sites while

restricting the access of most ER-resident proteins, including reticuloplasmins. Those resident proteins that inadvertently become removed from the ER are retrieved through retrograde Golgi vesicles (Kuehn and Schekman, 1997).

Figure 7 presents a hypothetical model illustrating the possible post-translational sorting pathway(s) of peroxisomal membrane (peroxisomal APX) and matrix (CAT-SKL) proteins in plant cells. Rather than using the general term "privileged site," we propose the term "peroxisomal ER subdomain" (pER). In Figure 7, cytosolic molecular chaperones are shown associated with nascent polypeptides because these chaperones seem to be involved in organelle acquisition of PMPs (Figure 6C) and matrix proteins (Crookes and Olsen, 1998; Pool et al., 1998). Although our data are meager for suggesting an initial sorting of matrix proteins mainly into putative transport vesicles rather than directly into preexisting peroxisomes, this alternative sorting pathway should be considered seriously in view of recent studies implicating ER and vesicular transport in peroxisomal biogenesis in plants and other organisms.

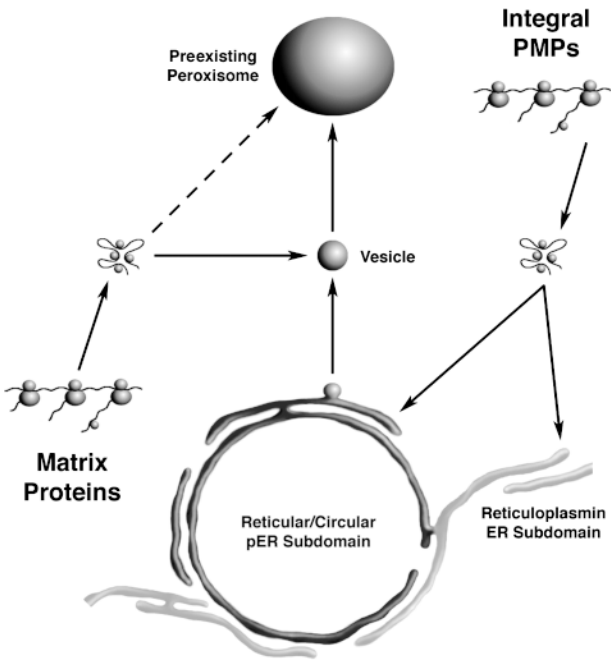

Figure 7. Model for the Sorting of Membrane and Matrix Proteins to Plant Peroxisomes.

Membrane and matrix proteins synthesized on cytosolic polysomes appear to interact with molecular chaperones before post-translational organelle sorting. PMPs (such as peroxisomal APX) may sort first to the reticuloplasmic-containing ER or to a peroxisomal ER (pER) subdomain (reticular/circular structure). Exit of PMPs from pER seems to involve vesicles that are subsequently sorted to preexisting peroxisomes (evidence from BFA experiments). Matrix proteins (with PTS1 or PTS2) also could sort indirectly (possibly to vesicles), or in some instances directly (dashed line), to preexisting peroxisomes.

Whether PMPs sort from the cytosol initially to an ER that possesses reticuloplasmins or to pER is not known. Our expectation is that they sort first to ER subdomains with the reticuloplasmins because these residents are involved in both post-translational and cotranslational uptake of proteins into the ER (Denecke et al., 1991; McClellan et al., 1998), and because Pex2p and Pex16p colocalize with Kar2p (a BiP homolog) in the ER of *Y. lipolytica* cells (Titorenko and Rachubinski, 1998b). If PMPs insert into reticuloplasmin ER, then they presumably move to and become localized within pER. Reticuloplasmins probably would be excluded from pER because they could not be retrieved by a peroxisomal retrograde vesicle system. The mechanisms for these latter processes are completely unknown.

Properly conceived and executed time-course studies clearly are needed to help resolve potential reticuloplasmin–peroxisomal APX interactions and to provide direct evidence for vesicular transport of PMPs from pER to peroxisomes. Such studies should provide meaningful modifications of the model in Figure 7. Meanwhile, that model serves not only as a base on which to test the validity of sorting pathways for peroxisomal proteins but also as a useful starting point for considering how peroxisomes differentiate (enlarge) and proliferate in plant cells.

METHODS

Plasmid Constructions

Molecular biology reagents were purchased from Promega (Madison, WI) or New England BioLabs (Beverly, MA), and standard recombinant DNA procedures were performed as described by Sambrook et al. (1989). All DNA mutagenesis reactions were performed by using polymerase chain reaction (PCR)–based site-directed mutagenesis, as described previously (Trelease et al., 1996b). Oligonucleotides for PCR were synthesized at the Arizona State University Bioresources Facility (Tempe, AZ). Sequences of all mutated DNAs were confirmed by nucleotide sequence analyses performed with an Applied Biosystems (Foster City, CA) Model 377 automated sequencer (Arizona State University Bioresources Facility).

pRLT2/HA-pAPX was constructed in the following manner. First, the EcoRI fragment of pGEM/PMP31 (DNA coding for the cottonseed peroxisomal ascorbate peroxidase [APX]; Bunkelmann and Trelease, 1996), containing the entire open reading frame (ORF) of APX and portions of the 5′ and 3′ APX untranslated regions (UTRs), was cloned into the EcoRI-digested mammalian expression vector pMT (Trelease et al., 1994), yielding pMT/pAPX. Next, pMT/HA-pAPX was generated by PCR-based mutagenesis. PCR mixtures included pMT/pAPX as template DNA, a reverse primer (5′-GCAACAACACCAGCAAGCTGG-3′) corresponding to a 21-bp region downstream of a unique SnaBI site in pAPX, and a forward primer (5′-GACTCTGCAGCCATGGGGTACCCT-TACGACGTCCCAGACTACGCTGCGTTTCCAGTAGTCGATACCGAG-3′) that introduced sequences in the 5′ UTR of peroxisomal APX coding for a translation initiation site (AUG), glycine linkers, and a single copy of the nine–amino acid hemagglutinin (HA) epitope (underlined, MGYPY-DVPDYAG) (Kolodziej and Young, 1991).

After PCR, DNA products were purified by affinity chromatography (Qiagen, Chatsworth, CA), ligated into the TA cloning vector pCR2.1 (Invitrogen, San Diego, CA), and then subcloned into PstI-SnaBI–digested pMT/pAPX, yielding pMT/HA-pAPX. Finally, the BglII-XbaI fragment of pMT/HA-pAPX, containing the entire coding region of peroxisomal APX plus DNA coding for the N-terminal-appended HA epitope tag and portions of the 5′ and 3′ APX UTRs, was ligated into the BamHI-XbaI–digested plant expression vector pRTL2ΔN/S (Lee et al., 1997), yielding pRTL2/HA-pAPX with a 35S cauliflower mosaic virus promoter.

pRLT2/CAT-pAPX, coding for the C-terminal 36–amino acid residues of peroxisomal APX and for a serine–arginine linker appended to the C terminus of the chloramphenicol acetyltransferase (CAT) ORF, was constructed as follows. A PCR mixture included pRTL2/pAPX as template DNA, a forward primer (5′-CCCACTTCAGCTCGCTCTAGAGTAATGGTGAAGG-3′) that modified the DNA sequences encoding lysine^{252} of APX to an arginine codon and introduced an XbaI site, and a reverse primer (5′-CGCATCTAGACGTTTCACTTCATTCTTTTGCGGACC-3′) that introduced an XbaI site in the 3′ UTR of pAPX. The resulting PCR DNA products were TA-cloned into pCR2.1 (generating pCR2.1/pAPX+36), digested with XbaI, and then ligated into XbaI-digested pRTL2/CAT-XbaI (a general-purpose CAT fusion cassette vector; Mullen et al., 1997b) yielding pRTL2/CAT-pAPX. Construction of pRTL2/CAT and pRTL2/CAT–Ser-Lys-Leu (CAT-SKL) has been described elsewhere (Trelease et al., 1996b; Lee et al., 1997). pBIN35Sβ60catE9′ was provided by François Chaumont (University of Louvain, Louvain-la-Neuve, Belgium) (Chaumont et al., 1994).

cDNA clones used for in vitro transcription/translation reactions were subcloned into pGEM7Z (Promega) in an orientation that allowed T7-driven transcription. pGEM/HA-pAPX was constructed by excising the EcoRI-EcoRI fragment of pMT/HA-pAPX and then ligating the fragment into EcoRI-digested pGEM7Z. pGEM/Pex15p was constructed by excising the EcoRI-HindIII fragment of p21.26 (provided by S. Subramani, University of California–San Diego, La Jolla) containing the entire ORF of *Saccharomyces cerevisiae* PMP Pex15p and portions of the 5′ and 3′ UTRs (Elgersma et al., 1997). The EcoRI-HindIII fragment was ligated into EcoRI-HindIII–digested pGEM7Z, yielding pGEM/Pex15p. pGEM/PMP47 was constructed by ligating the EcoRI-BamHI fragment of pEX (provided by Joel Goodman, University of Texas Southwestern Medical Center, Dallas) containing the entire ORF of *Candida boidinii* peroxisomal membrane protein (PMP) 47 and portions of the 5′ and 3′ UTRs (Dyer et al., 1996) into EcoRI-BamHI–digested pGEM7Z. pGEM/VAMP2 was constructed by ligating the XbaI-NheI fragment of pTW2 (provided by J. McNew, Memorial Sloan-Kettering Cancer Center, New York) containing the entire ORF of mouse brain synaptobrevin/vesicle-associated membrane protein 2 (VAMP2), an appended C-terminal histidine$_6$-tag, and portions of the 5′ and 3′ UTRs (Weber et al., 1998) into XbaI-digested pGEM7Z.

Cell Culture, Microprojectile Bombardment, and Brefeldin A Treatments

Tobacco (*Nicotiana tabacum* cv Bright Yellow 2) (BY-2) suspension cultures were grown as described previously (Banjoko and Trelease, 1995). BY-2 cells were collected 4 days after subculture and resuspended in an equal volume of transformation medium (growth medium without 2,4-D, plus 250 mM sorbitol and 250 mM mannitol) (Banjoko and Trelease, 1995; Lee et al., 1997). For transient transformation, cells were spread on filter papers premoistened with transformation medium, and after a 1-hr equilibration, were bombarded with 10 μg of plasmid DNA through means of a biolistic particle delivery system as described by Flynn et al. (1998). Cells were allowed to transiently express gene products for 4 to 20 hr, depending on the experiment. Approximately 0.5 to 2% of the cells collected from the plates were transformed transiently.

Brefeldin A (BFA) (Molecular Probes, Eugene, OR) was dissolved in DMSO (Fisher) (10 mg/mL stock solution) and used at a final concentration of 100 μg/mL in transformation medium. Collected cells were resuspended in an equal volume of transformation medium plus BFA, spread on filter papers premoistened with this medium, bombarded, and incubated in the same plates in darkness (room temperature); after 4 to 10 hr, they were scraped from the plates, fixed in formaldehyde, and processed for immunofluorescence microscopy. In a control experiment, medium plus an appropriate amount of DMSO was used for all steps through bombardment. For recovery experiments, cells bombarded in the presence of BFA were incubated for 8 to 10 hr with BFA, scraped from filter papers, washed twice in medium minus BFA, spread on filter papers with medium minus BFA, and incubated for an additional 8 to 10 hr before fixation in formaldehyde.

Immunofluorescence Microscopy

After fixation in 4% (w/v) formaldehyde and 0.5 × transformation medium for 1 hr, cells were washed in phosphate-buffered saline (PBS) and incubated in 0.1% (w/v) pectoylase Y-23 in PBS for 2 hr at 30°C. Plasma and organellar membranes were permeabilized by incubating the cells in 0.3% (v/v) Triton X-100 in PBS for 15 min at room temperature (Lee et al., 1997). Applications of primary and fluorescent dye–conjugated secondary antibodies to 1 mL of cells in 1.5-mL microcentrifuge tubes were performed as described previously (Trelease et al., 1996a, 1996b). Antibody sources and concentrations used were as follows (affinity-purified refers to IgGs in antiserum that were affinity-bound and then acid-released from protein A–Sepharose in columns, as described by Kunce et al., 1988): rabbit anti-cucumber peroxisomal APX affinity-purified IgGs (1:500) (Corpas et al., 1994); rabbit anti-cottonseed catalase affinity-purified IgGs (1:500) (Kunce et al., 1988); rabbit anti-CAT affinity-purified IgGs (1:500) (5′→3′, Boulder, CO); rabbit anti-castor calnexin antiserum (1:500) and rabbit anti-castor calreticulin antiserum (1:500), both provided by S. Coughlan (Coughlan et al., 1997); rabbit anti-maize binding protein (BiP) antiserum (1:500), provided by R. Boston (Fontes et al., 1991); rabbit anti-pea reversibly glycosylated polypeptide (RGP1) antiserum (1:500), provided by K. Dhugga (Dhugga et al., 1997); rabbit anti-peptide δ tonoplast intrinsic protein (δ-TIP) antiserum (1:200), a gift from J. Rogers (Jauh et al., 1998); mouse anti-CAT monoclonal antibody (undiluted hybridoma medium), provided by S. Subramani; mouse anti-HA epitope monoclonal antibody (1:300) (Boehringer Mannheim); mouse anti-maize β-ATPase E monoclonal antibody (1:10), provided by T. Elthon (Luethy et al., 1993); goat anti-rabbit rhodamine (1:500); goat anti-rabbit cyanine 5 (Cy5) (1:500); goat anti-mouse Cy5 (1:500); goat anti-rabbit Cy2 (1:1000); goat anti-mouse Cy2 (1:500 or 1:2000); and goat anti-mouse Cy3 (1:2000). All fluorescent dye-conjugated secondary antibodies were purchased from Jackson ImmunoResearch Labs, Inc. (Westgrove, PA).

For staining with 3,3′-dihexyloxacarbocyanine iodide (DiOC$_6$; Molecular Probes), living cells equilibrated in transformation medium or cells fixed in formaldehyde and treated with pectolyase and Triton X-100 were incubated in a 1:1000 or 1:300 dilution (in PBS),

respectively, of a 1 mg/mL $DiOC_6$ stock solution (in DMSO) for 10 min at room temperature. When fixed cells were also labeled with antibodies, $DiOC_6$ was added during the final 10 min of incubation in PBS with the secondary antibodies.

Labeled cells were mounted on glass slides in 90% glycerol with *n*-propyl gallate (Sigma) to prevent photobleaching of fluorescence, then viewed with either a Zeiss Axiovert 100 epifluorescence microscope (Carl Zeiss Inc., Thornwood, NY) or a Leica DM RBE microscope equipped with a Leica TCS NT confocal scanning head (Leica, Heidelberg, Germany). Epifluorescence images were photographed with TMAX 400 ASA black and white film (Eastman Kodak), and printed images were computer-scanned and subsequently composed into figures by using Adobe Photoshop 3.0. For confocal laser scanning microscopy, fluorophores were excited with a 488-nm argon ion laser (Cy2 and $DiOC_6$) or a 633-nm helium/neon laser (Cy5) passed through a triple dichroic mirror (TD 488/568/633) and attenuated to 15% (for $DiOC_6$) or 75 to 95% (Cy2 and Cy5) maximal emission. Cy2 or $DiOC_6$ and Cy5 emissions were separated with bandpass 530/30-nm and long-pass 645-nm filters, respectively. Fluorophore emissions were collected simultaneously in double-labeling experiments; single-labeling experiments showed no detectable crossover at the settings used for data collection. All confocal images were acquired as z-series of representative cells with the Leica TCS NT software package (version 1.5.451); at least 20 transformed cells were examined for each experiment. Single optical sections were selected from each z-series and saved as 512 × 512-pixel digital images, which were later adjusted for contrast and brightness, pseudocolored green or red, and then composed into figures (Figures 2 to 4) by using Adobe Photoshop 3.0.

Organelle Membrane Preparations

Microsomal-derived endoplasmic reticulum (ER) membranes (MEMs) were prepared from cultured maize (*Zea mays* inbred A636) endosperm cells by methods described by Riedell and Miernyk (1988) and Shatters and Miernyk (1991). Briefly, cells were homogenized with a mortar and pestle, and a pellet was obtained after ultracentrifugation at 100,000*g* for 60 min. MEMs were purified from this microsomal pellet by equilibration of rough vesicles in a linear 15 to 45% (w/w) sucrose gradient. Vesicles collected from the gradient were further purified by gel permeation chromatography (Sepharose CL-4B).

Replicate assays for organelle marker enzymes and proteins were conducted in a balance sheet fashion (Table 1). Plasma membrane vesicles were prepared from the same cultured cells by using the aqueous two-phase partitioning method of Larsson et al. (1994). Potatoes (*Solanum tuberosum*; small, "red skinned") were obtained from a local market, and peroxisomes were purified by using a modification of the Percoll gradient method described by Neuburger et al. (1982). Purified peroxisomes were ruptured osmotically, and membranes were collected in a 100,000*g* (60 min) pellet. Mitochondria and chloroplasts were isolated from 14-day, light-grown pea (*Pisum sativum* cv Little Marvel) seedlings (Fang et al., 1987). The purified organelles were osmotically ruptured, and the membranes were pelleted as described above for peroxisomal membranes. The plastid envelope–enriched fraction was prepared as described by Cline (1986). A fraction enriched in mitochondrial outer membrane vesicles was isolated as described by Miernyk and Dennis (1983). All subcellular fractions obtained for each organelle isolation were evaluated for the amount of contaminating marker enzymes by following described procedures, or as referenced by Riedell and Miernyk (1988).

In Vitro Transcription/Translations, Membrane Protein Associations, and Immunoremoval of Molecular Chaperones

Coupled transcription/translation was accomplished by using the Promega T7 TNT coupled reticulocyte lysate system according to the manufacturer's instructions. Translation-grade L-^{35}S-methionine (>37 TBq/mmol) was purchased from DuPont New England Nuclear (Boston, MA). Cotranslational membrane association reactions (100 μL) contained MEMs equivalent to 1 mg of total protein (Shatters and Miernyk, 1991; Miernyk et al., 1992). For post-translational membrane association reactions, translations were continued for 1 hr and then terminated by the addition of emetine (Sigma) or RNase to a final concentration of 50 μM. Ribosomes were removed by centrifugation at 150,000*g* for 15 min at 4°C in a Beckman (Palo Alto, CA) Model TLA 100.2 rotor.

Membrane association of radiolabeled proteins was measured after washing MEMs with 300 mM KCl on ice for 30 min. ATP was removed from the translation mixtures by adding 5 to 10 units (μmol min^{-1}) of apyrase (Sigma). Membrane integration was determined by washing with alkaline sodium carbonate, as described by Corpas et al. (1994). Membrane pellets and the proteins solubilized by the various treatments were acid precipitated, washed, and analyzed by SDS-PAGE plus radioanalytical imaging (Shatters and Miernyk, 1991; Miernyk et al., 1992).

For experiments involving immunoremoval of chaperones, in vitro transcription/translation was conducted as described above, except that a Promega wheat germ system was used instead of reticulocyte lysate. Wheat germ supernatants were depleted of heat shock protein (Hsp70) by addition of anti–Hsp-70 antibodies before the initiation of translation (additions of mRNA and ^{35}S-methione), as described previously by Miernyk et al. (1992). Immunoremoval of the YdJ1 class of cytoplasmic DnaJ homolog used the same procedures as for removal of Hsp70, except that the antiserum used was that described by Zhou et al. (1995). Immunoremoval of cytoplasmic nucleotide exchange factor was performed by using rabbit polyclonal antiserum raised against the recombinant AtE1 protein (GenBank accession number U64825) (B. Kroczynska and J.A. Miernyk, unpublished data). Monoclonal antibodies against the E1α subunit of pyruvate dehydrogenase have been described elsewhere (Luethy et al., 1995).

ACKNOWLEDGMENTS

We thank all those who provided us with their generous gifts of plasmids and antibodies that were used in this study. Special thanks are extended to Dr. John Dyer (U.S. Department of Agriculture, Agricultural Research Service, Southern Regional Research Center, New Orleans, LA) for his insightful discussions of experimental results and for a thorough reading of the manuscript. Maho Uchida maintained the BY-2 cell cultures. Confocal imaging and data analyses were conducted in the W.M. Keck BioImaging Laboratory at Arizona State University. The research was supported by National Science Foundation Grant MCB-9728935 to R.N.T. and in part by the William N. and Myriam Pennington Foundation. The Molecular and Cellular Biology Program at Arizona State University provided some research assistantship support for C.S.L.

Received June 22, 1999; accepted September 6, 1999.

REFERENCES

Aridor, M., Weissman, J., Bannykh, S., Nuoffer, C., and Balch, W.E. (1998). Cargo selection by the COPII budding machinery during export from the ER. J. Cell Biol. **141,** 61–70.

Baerends, R.J.S., Rasmussen, S.W., Hilbrands, R.E., van der Heide, M., Faber, K.N., Reuvekamp, P.T.W., Kiel, J.A.K.W., Cregg, J.M., van der Klei, I.J., and Veenhuis, M. (1996). The *Hansenula polymorpha PER9* gene encodes a peroxisomal membrane protein essential for peroxisome assembly and integrity. J. Biol. Chem. **271,** 8887–8894.

Baker, A. (1996). Biogenesis of plant peroxisomes. In Membranes: Specialized Functions in Plants, M. Smallwood, J.P. Know, and D.J. Bowels, eds (Oxford, UK: BioScientific), pp. 421–440.

Ballard, J.L., Dyer, J.M., Pelosof, L.C., Gowani, J.W., and Goodman, J.M. (1998). Aberrant peroxisomes in a mutant deficient in a mPTS-binding protein. Mol. Biol. Cell **9** (suppl.), 2023.

Banjoko, A., and Trelease, R.N. (1995). Development and application of an in vivo plant peroxisome import system. Plant Physiol. **107,** 1201–1208.

Bodnar, A.G., and Rachubinski, R.A. (1991). Characterization of the integral membrane polypeptides of rat liver peroxisomes isolated from untreated and clofibrate-treated rats. Biochem. Cell Biol. **69,** 499–508.

Brickner, D.G., Brickner, J.H., and Olsen, L.J. (1998). Sequence analysis of a cDNA encoding Pex5p, a peroxisomal targeting signal type 1 receptor from *Arabidopsis* (accession no. AF074843) (PGR-98-154). Plant Physiol. **118,** 330.

Bukau, B., and Horwich, A.L. (1998). The Hsp70 and Hsp60 chaperone machines. Cell **92,** 351–366.

Bunkelmann, J., and Trelease, R.N. (1996). Ascorbate peroxidase: A prominent membrane protein in oilseed glyoxysomes. Plant Physiol. **110,** 589–598.

Chaumont, F., de Castro Silva Filho, M., Thomas, D., Leterme, S., and Boutry, M. (1994). Truncated presequences of mitochondrial F_1-ATPase β subunit from *Nicotiana plumbaginifolia* transport CAT and GUS proteins into mitochondria of transgenic tobacco. Plant Mol. Biol. **24,** 631–641.

Cline, K. (1986). Import of proteins into chloroplasts. Membrane integration of a thylakoid precursor protein reconstituted in chloroplast lysates. J. Biol. Chem. **261,** 14804–14810.

Corpas, F.J., and Trelease, R.N. (1997). The plant 73 kDa peroxisomal membrane protein (PMP73) is immunorelated to molecular chaperones. Eur. J. Cell Biol. **73,** 49–57.

Corpas, F.J., and Trelease, R.N. (1998). Differential expression of ascorbate peroxidase and a putative molecular chaperone in the boundary membrane of differentiating cucumber seedling peroxisomes. J. Plant Physiol. **153,** 332–338.

Corpas, F.J., Bunkelmann, J., and Trelease, R.N. (1994). Identification and immunochemical characterization of a family of peroxisome membrane proteins (PMPs) in oilseed glyoxysomes. Eur. J. Cell Biol. **65,** 280–290.

Coughlan, S.J., Hastings, C., and Winfrey, R. (1997). Cloning and characterization of the calreticulin gene from *Ricinus communis* L. Plant Mol. Biol. **34,** 897–911.

Crofts, A.J., and Denecke, J. (1998). Calreticulin and calnexin in plants. Trends Plant Sci. **3,** 396–399.

Crookes, W.J., and Olsen, L.J. (1998). The effects of chaperones and the influence of protein assembly on peroxisomal protein import. J. Biol. Chem. **273,** 17236–17242.

Denecke, J., Goldman, M.H.S., Demolder, J., Seurinck, J., and Botterman, J. (1991). The tobacco luminal binding protein is encoded by a multigene family. Plant Cell **3,** 1025–1035.

Denecke, J., Carlsson, L.E., Vidal, S., Höglund, A.-S., Ek, B., van Zeijl, M.J., Sinjorgo, K.M.C., and Palva, E.T. (1995). The tobacco homolog of mammalian calreticulin is present in protein complexes in vivo. Plant Cell **7,** 391–406.

Dhugga, K.S., Tiwari, S.C., and Ray, P.M. (1997). A reversibly glycosylated polypeptide (RGP1) possibly involved in plant cell wall synthesis: Purification, gene cloning, and *trans*-Golgi localization. Proc. Natl. Acad. Sci. USA **94,** 7679–7684.

Distel, B., et al. (1996). A unified nomenclature for peroxisome biogenesis factors. J. Cell Biol. **135,** 1–3.

Dyer, J.M., McNew, J.A., and Goodman, J.M. (1996). The sorting sequence of the peroxisomal integral membrane protein PMP47 is contained within a short hydrophilic loop. J. Cell Biol. **133,** 269–280.

Elgersma, Y., Kwast, L., van de Berg, M., Snyder, W.B., Distel, B., Subramani, S., and Tabak, H.F. (1997). Overexpression of Pex15p, a phosphorylated peroxisomal integral membrane protein required for peroxisome assembly in *S. cerevisiae*, causes proliferation of the endoplasmic reticulum membrane. EMBO J. **16,** 7326–7341.

Erdmann, R., Veenhuis, M., and Kunau, W.-H. (1997). Peroxisomes: Organelles at the crossroads. Trends Cell Biol. **7,** 400–407.

Faber, K.N., Heyman, J.A., and Subramani, S. (1998). Two AAA family peroxins, PpPex1p and PpPex6p, interact with each other in an ATP-dependent manner and are associated with different subcellular membranous structures distinct from peroxisomes. Mol. Cell. Biol. **18,** 936–943.

Fang, T.K., David, N.R., Miernyk, J.A., and Randall, D.D. (1987). Isolation and purification of functional pea leaf mitochondria free of chlorophyll contamination. Curr. Top. Plant Biochem. Physiol. **6,** 175.

Flynn, C.R., Mullen, R.T., and Trelease, R.N. (1998). Mutational analyses of a type 2 peroxisomal targeting signal that is capable of directing oligomeric protein import into tobacco BY-2 glyoxysomes. Plant J. **16,** 709–720.

Fontes, E.B.P., Shank, B.B., Wrobel, R.L., Moose, S.P., O'Brian, G.R., Wurtzel, E.T., and Boston, R.S. (1991). Characterization of an immunoglobulin binding protein homolog in the maize *floury-2* endosperm mutant. Plant Cell **3,** 483–496.

Frydman, J., Nimmesgern, E., Ohtsuka, K., and Hartl, F.U. (1994). Folding of nascent polypeptide chains in a high molecular mass assembly with molecular chaperones. Nature **370,** 111–117.

Gietl, C. (1996). Protein targeting and import into plant peroxisomes. Physiol. Plant. **97,** 599–608.

Hannan, L.A., and Edidin, M. (1996). Traffic, polarity, and detergent solubility of a glycosylphosphatidylinositol-anchored protein after LDL-deprivation of MDCK cells. J. Cell Biol. **133,** 1265–1276.

Hepler, P.K., Palevitz, B.A., Lancelle, S.A., McCauley, M.M., and Lichtscheidl, I. (1990). Cortical endoplasmic reticulum in plants. J. Cell Sci. **96,** 355–373.

Hettema, E.H., Ruigrok, C.C.M., Koerkamp, M.G., van den Berg, M., Tabak, H.F., Distel, B., and Braakman, I. (1998). The cytosolic

DnaJ-like protein Djp1p is involved specifically in peroxisomal protein import. J. Cell Biol. **142,** 421–434.

Hobman, T.C., Zhao, B., Chan, H., and Farquhar, M.G. (1998). Immunoisolation and characterization of a subdomain of the endoplasmic reticulum that concentrates proteins involved in COPII vesicle biogenesis. Mol. Biol. Cell **9,** 1265–1278.

Horng, J.-T., Behari, R., Burke, L.E.C.-A., and Baker, A. (1995). Investigation of the energy requirement and targeting signal for the import of glycolate oxidase into glyoxysomes. Eur. J. Biochem. **230,** 157–163.

Huang, A.H.C., Trelease, R.N., and Moore, T.S. (1983). Plant Peroxisomes. American Society of Plant Physiologists Monograph Series. (New York: Academic Press).

Imanaka, T., Shiina, Y., Takano, T., Hashimoto, T., and Osumi, T. (1996). Insertion of the 70-kDa peroxisomal membrane protein into peroxisomal membranes in vivo and in vitro. J. Biol. Chem. **271,** 3706–3713.

Ishikawa, T., Yoshimura, K., Sakai, K., Tamoi, M., Takeda, T., and Shigeoka, S. (1998). Molecular characterization and physiological role of glyoxysome-bound ascorbate peroxidase from spinach. Plant Cell Physiol. **39,** 23–34.

Jauh, G.-Y., Fischer, A.M., Grimes, H.D., Ryan, C.A., and Rogers, J.C. (1998). δ–Tonoplast intrinsic protein defines unique plant vacuole functions. Proc. Natl. Acad. Sci. USA **95,** 12995–12999.

Just, W.W., and Diestelkötter, P. (1996). Protein insertion into the peroxisomal membrane. Ann. N.Y. Acad. Sci. **804,** 60–75.

Kammerer, S., Holzinper, A., Welsch, U., and Roscher, A.A. (1998). Cloning and characterization of the gene encoding the human peroxisomal assembly protein Pex3p. FEBS Lett. **429,** 53–60.

Klausner, R.D., Donaldson, J.G., and Lippincott-Schwartz, J. (1992). Brefeldin A: Insights into the control of membrane traffic and organelle structure. J. Cell Biol. **116,** 1071–1080.

Kolodziej, P.A., and Young, R.A. (1991). Epitope tagging and protein surveillance. Methods Enzymol. **194,** 508–519.

Kragler, F., Lametschwandtner, G., Christmann, J., Hartig, A., and Harada, J.J. (1998). Identification and analysis of the plant peroxisomal targeting signal 1 receptor NtPEX5. Proc. Natl. Acad. Sci. USA **95,** 13336–13341.

Kuehn, M.J., and Schekman, R. (1997). COPII and secretory cargo capture into transport vesicles. Curr. Opin. Cell Biol. **9,** 477–483.

Kunau, W.-H., and Erdmann, R. (1998). Peroxisome biogenesis: Back to the endoplasmic reticulum? Curr. Biol. **8,** 299–302.

Kunce, C.M., Trelease, R.N., and Turley, R.B. (1988). Purification and biosynthesis of cottonseed (*Gossypium hirsutum* L.) catalase. Biochem. J. **251,** 147–155.

Kutay, U., Ahnert-Hilger, G., Hartmann, E., Wiedenmann, B., and Rapoport, T.A. (1995). Transport route for synaptobrevin via a novel pathway of insertion into the endoplasmic reticulum membrane. EMBO J. **14,** 217–223.

Larsson, C., Sommarin, M., and Widell, S. (1994). Isolation of highly purified plant plasma membranes and the separation of inside-out and right-side-out vesicles. Methods Enzymol. **228,** 452–469.

Lee, M.S., Mullen, R.T., and Trelease, R.N. (1997). Oilseed isocitrate lyases lacking their essential type 1 peroxisomal targeting signal are piggybacked to glyoxysomes. Plant Cell **9,** 185–197.

Lin, Y., Sun, L., Nguyen, L.V., Rachubinski, R.A., and Goodman, H.M. (1999). The Pex16p homolog SSE1 and storage organelle formation in *Arabidopsis* seeds. Science **284,** 328–330.

Luethy, M.H., Horak, A., and Elthon, T.E. (1993). Monoclonal antibodies to the alpha and beta-subunits of the plant mitochondrial F_1-ATPase. Plant Physiol. **101,** 931–937.

Luethy, M.H., David, N.R., Elthon, T.E, Miernyk, J.A., and Randall, D.D. (1995). Characterization of a monoclonal antibody directed against the E1α subunit of plant pyruvate dehydrogenase. J. Plant Physiol. **145,** 443–449.

McCammon, M.T., McNew, J.A., Willy, P.J., and Goodman, J.M. (1994). An internal region of the peroxisomal membrane protein PMP47 is essential for sorting to peroxisomes. J. Cell Biol. **124,** 915–925.

McCauley, M.M., and Hepler, P.K. (1990). Visualization of the endoplasmic reticulum in living buds and branches of the moss *Funaria hygrometrica* by confocal laser scanning microscopy. Development **109,** 753–764.

McClellan, A.J., Endres, J.B., Vogel, J.P., Palazzi, D., Rose, M.D., and Brodsky, J.L. (1998). Specific molecular chaperone interactions and an ATP-dependent conformational change are required during posttranslational protein translocation into the yeast ER. Mol. Biol. Cell **9,** 3533–3545.

Miernyk, J.A., and Dennis, D.T. (1983). Mitochondrial, plastid and cytosolic isozymes of hexokinase in endosperm of *Ricinus communis.* Arch. Biochem. Biophys. **226,** 458–468.

Miernyk, J.A., Duck, N.B., Shatters, R.G., Jr., and Folk, W.R. (1992). The 70-kilodalton heat shock cognate can act as a molecular chaperone during the membrane translocation of a plant secretory protein precursor. Plant Cell **4,** 821–829.

Mullen, R.T., and Trelease, R.N. (1996). Biogenesis and membrane properties of peroxisomes: Does the boundary membrane serve and protect? Trends Plant Sci. **1,** 389–394.

Mullen, R.T., Lee, M.S., Flynn, C.R., and Trelease, R.N. (1997a). Diverse amino acid residues function within the type 1 peroxisomal targeting signal. Implication for the role of accessory residues upstream of the type 1 peroxisomal targeting signal. Plant Physiol. **115,** 881–889.

Mullen, R.T., Lee, M.S., and Trelease, R.N. (1997b). Identification of the peroxisomal targeting signal for cottonseed catalase. Plant J. **12,** 313–322.

Napier, R.M., Trueman, S., Henderson, J., Boyce, J.M., Hawes, C., Fricker, M.D., and Venis, M.A. (1995). Purification, sequencing and functions of calreticulin from maize. J. Exp. Bot. **46,** 1603–1613.

Neuburger, M., Journet, E.-P., Bligny, R., Carde, J.-P., and Douce, R. (1982). Purification of plant mitochondria by isopycnic centrifugation in density gradients of Percoll. Arch. Biochem. Biophys. **217,** 312–323.

Neuhaus, J.-M., and Rogers, J.C. (1998). Sorting of proteins to vacuoles in plant cells. Plant Mol. Biol. **38,** 127–144.

Okita, T.W., and Rogers, J.C. (1996). Compartments of proteins in the endomembrane system of plant cells. Annu. Rev. Plant Physiol. Plant Mol. Biol. **47,** 327–350.

Olsen, L.J. (1998). The surprising complexity of peroxisome biogenesis. Plant Mol. Biol. **38,** 163–189.

Patterson, W.R., and Poulos, T.L. (1995). Crystal structure of recombinant pea cytosolic ascorbate peroxidase. Biochemistry **34,** 4331–4341.

Pause, B., Diestelkötter, P., Heid, H., and Just, W.W. (1997). Cytosolic factors mediate protein insertion into the peroxisomal membrane. FEBS Lett. **414,** 95–98.

Pool, M.R., López-Huertas, E., and Baker, A. (1998). Characterization of intermediates in the process of plant peroxisomal protein import. EMBO J. **17,** 6854–6862.

Riedell, W.E., and Miernyk, J.A. (1988). Glycoprotein synthesis in maize endosperm cells. The nucleotide diphosphate-sugar: Dolicholphosphate glycosyltransferases. Plant Physiol. **87,** 420–426.

Sabnis, R.W., Deligeorgiev, T.G., Jachak, M.N., and Dalvi, T.S. (1997). $DiOC_6(3)$: A useful dye for staining the endoplasmic reticulum. Biotechnol. Histochem. **72,** 253–258.

Salomons, F.A., van der Klei, I.J., Kram, A.M., Harder, W., and Veenhuis, M. (1997). Brefeldin A interferes with peroxisomal protein sorting in the yeast *Hansenula polymorpha.* FEBS Lett. **411,** 133–139.

Sambrook, J., Fritsch, E.F., and Maniatis, T. (1989). Molecular Cloning: A Laboratory Manual, 2nd ed. (Cold Spring Harbor, NY: Cold Spring Harbor Laboratory Press).

Satiat-Jeunemaitre, B., Cole, L., Bourett, T., Howard, R., and Hawes, C. (1996). Brefeldin A effects in plants and fungal cells: Something new about vesicle trafficking? J. Microsc. **181,** 162–177.

Schumann, U., Gietl, C., and Schmid, M. (1999). Sequence analysis of a cDNA encoding Pex10p, a zinc-binding peroxisomal integral membrane protein from Arabidopsis (accession no. AF119572) (PGR 99-025). Plant Physiol. **119,** 1147.

Shatters, R.G., Jr., and Miernyk, J.A. (1991). A zein signal sequence functions as a signal-anchor when fused to maize alcohol dehydrogenase. Biochim. Biophys. Acta **1068,** 179–188.

Sitia, R., and Meldolesi, J. (1992). Endoplasmic reticulum: A dynamic patchwork of specialized subregions. Mol. Biol. Cell **3,** 1067–1072.

Staehelin, L.A. (1997). The plant ER: A dynamic organelle composed of a large number of discrete functional domains. Plant J. **11,** 1151–1165.

Staehelin, L.A., and Driouich, A. (1997). Brefeldin A effects in plants. Plant Physiol. **114,** 401–403.

Subramani, S. (1998). Components involved in peroxisome import, biogenesis, proliferation, turnover, and movement. Physiol. Rev. **78,** 171–188.

Terasaki, M. (1993). Probes for the endoplasmic reticulum. In Fluorescent and Luminescent Probes for Biological Activity, W.G. Madson, ed (London: Academic Press), pp. 120–123.

Titorenko, V.I., and Rachubinski, R.A. (1997). Import of some matrix and membrane proteins into peroxisomes of the yeast *Yarrowia lipolytica* can occur via endoplasmic reticulum–derived vesicles. In Yeast Cell Biology, T.N. Davis, M.D. Rose, and T. Stevens, eds (Cold Spring Harbor, NY: Cold Spring Harbor Laboratory Press), p. 220.

Titorenko, V.I., and Rachubinski, R.A. (1998a). The endoplasmic reticulum plays an essential role in peroxisome biogenesis. Trends Biol. Sci. **23,** 231–233.

Titorenko, V.I., and Rachubinski, R.A. (1998b). Mutants of the yeast *Yarrowia lipolytica* defective in protein exit from the endoplasmic reticulum are also defective in peroxisome biogenesis. Mol. Cell. Biol. **18,** 2789–2803.

Titorenko, V.I., Ogrydziak, D.M., and Rachubinski, R.A. (1997). Four distinct secretory pathways serve protein secretion, cell surface growth, and peroxisome biogenesis in the yeast *Yarrowia lipolytica.* Mol. Cell. Biol. **17,** 5210–5226.

Trelease, R.N., Choe, S.M., and Jacobs, B.L. (1994). Conservative amino acid substitutions of the C-terminal tripeptide (ARM) on cottonseed (*Gossypium hirsutum* L.) isocitrate lyase preserve import in vivo into mammalian cell peroxisomes. Eur. J. Cell Biol. **65,** 269–279.

Trelease, R.N., Lee, M.S., Banjoko, A., and Bunkelmann, J. (1996a). C-terminal polypeptides are necessary and sufficient for in vivo targeting of transiently-expressed proteins to peroxisomes in suspension-cultured plant cells. Protoplasma **195,** 156–167.

Trelease, R.N., Xie, W., Lee, M.S., and Mullen, R.T. (1996b). Rat liver catalase is sorted to peroxisomes by its C-terminal tripeptide Ala-Asn-Leu, not by the internal Ser-Lys-Leu motif. Eur. J. Cell Biol. **71,** 248–258.

Tugal, H.B., Pool, M., and Baker, A. (1999). Arabidopsis 22-kilodalton peroxisomal membrane protein. Nucleotide sequence analysis and biochemical characterization. Plant Physiol. **20,** 309–320.

Vergeres, G., Yen, T., Aggeler, J., Lausier, J., and Waskell, L. (1993). A model system for studying membrane biogenesis. Overexpression of cytochrome b_5 in yeast results in marked proliferation of the intracellular membranes. J. Cell Sci. **106,** 249–259.

Walton, P.A., Wendland, M., Subramani, S., Rachubinski, R.A., and Welch, W.J. (1994). Involvement of 70 kD heat-shock proteins in peroxisomal import. J. Cell Biol. **125,** 1037–1046.

Weber, T., Zemelman, B.V., McNew, J.A., Westermann, B., Gmachl, M., Parlati, F., Sollner, T.H., and Rothman, J.E. (1998). SNAREpins: Minimal machinery for membrane fusion. Cell **92,** 759–772.

Wimmer, C., Schmid, M., Veenhuis, M., and Gietl, C. (1998). The plant PTS1 receptor: Similarities and differences to its human and yeast counterparts. Plant J. **16,** 453–464.

Wright, R., Basson, M., D'Ari, L., and Rine, J. (1988). Increased amounts of HMG–CoA reductase induce "karmellae": A proliferation of stacked membrane pairs surrounding the yeast nucleus. J. Cell Biol. **107,** 101–114.

Yamaguchi, K., Mori, H., and Nishimura, M. (1995). A novel isoenzyme of ascorbate peroxidase localized on glyoxysomal and leaf peroxisomal membranes in pumpkin. Plant Cell Physiol. **36,** 1157–1162.

Zhang, H., Wang, J., Nickel, U., Allen, R.D., and Goodman, H.M. (1997). Cloning and expression of an *Arabidopsis* gene encoding a putative peroxisomal ascorbate peroxidase. Plant Mol. Biol. **34,** 967–971.

Zhou, R., Kroczynska, B., Hayman, G.T., and Miernyk, J. (1995). AtJ2, an *Arabidopsis* homolog of *Escherichia coli* DnaJ. Plant Physiol. **108,** 821–822.